ISPRS Journal of Photogrammetry and Remote Sensing 202 (2023) 334–355

Contents lists available at ScienceDirect

ISPRS Journal of Photogrammetry and Remote Sensing

journal homepage: www.elsevier.com/locate/isprsjprs

CropSow: An integrative remotely sensed crop modeling framework for field-level crop planting date estimation

Yin Liu, Chunyuan Diao *, Zijun Yang

Department of Geography and Geographic Information Science, University of Illinois at Urbana-Champaign, Urbana, IL 61801, USA

ARTICLE INFO

Keywords:
Planting date
Remote sensing
Crop growth model
Phenology

ABSTRACT

Crop planting timing is critical in regulating environmental conditions of crop growth throughout the season, and is an essential parameter in crop simulation models for estimating dry matter accumulation and yields. Accurate planting date information is key to characterizing crop growing dynamics under varying farming practices and facilitating agricultural adaptation to climate change. To date, the main methods to acquire planting dates include field survey methods, weather-dependent methods, and remote sensing phenological detecting methods. However, it is still challenging to effectively estimate the crop planting dates at field levels due to the lack of appropriate field-level modeling design as well as the dearth of ground planting reference data. In our study, we develop a novel CropSow modeling framework to estimate field-level planting dates by integrating the remote sensing phenological detecting method with the crop growth model. The remote sensing phenological detecting method is devised to retrieve the critical crop phenological metrics of farm fields from remote sensing time series, which are then integrated into the crop growth model for field planting date estimation in consideration of soil-crop-atmosphere continuum. CropSow leverages the rich physiological knowledge embedded in the crop growth model to scalably interpret satellite observations under a variety of environmental and management conditions for field-level planting date retrievals. With corn in Illinois, US as a case study, the developed CropSow outperforms three advanced benchmark models (i.e., the remote sensing accumulative growing degree day method, the weather-dependent method, and the shape model) in crop planting date estimation at the field level, with R square higher than 0.68, root mean square error (RMSE) lower than 10 days, and mean bias error (MBE) around 5 days from 2016 to 2020. It achieves better generalization performance than the benchmark models, as well as stronger adaptability to abnormal weather conditions with more robust performance in estimating the planting dates of farm fields. CropSow holds considerable promise to extrapolate over space and time for estimating the timing of crop planting of individual farm fields at large scales.

1. Introduction

Food security will be increasingly challenged in the upcoming years with the world's population growth, the growing scarcity of farmland, the changing consumption patterns, as well as the changing climate (Beddington, 2010). By 2050, 60 percent more food will need to be produced to feed a projected world population of 9.3 billion. Under these projected changing scenarios, adaptations of crop management practices are expected to be imperative in dealing with food security issues (Challinor et al., 2014). As one of the major crop management practices in determining the crop yield potential, the timing of crop planting plays a critical role in initializing the climatic and environmental conditions of crop growth and phenological development throughout the season (Baum et al., 2020). The adaptive management of crop planting can potentially mitigate the negative effects of heat or chilling stress on crop production, leading to substantial reduction in yield losses under future climate (Baum et al., 2020; Shew et al., 2020; Huang et al., 2020). In addition, planting date is an essential input variable of process-based crop growth models to estimate crop yields and assess food security prospects over space and time. Monitoring the timing of crop planting at field levels can largely facilitate the assessment of the gaps between achieved and achievable yields to enable more profitable and sustainable farm management adaptations (Jain et al., 2016).

Currently, the major methods of acquiring field-level planting date information can be divided into three categories: (1) field survey

* Corresponding author.
E-mail address: chunyuan@illinois.edu (C. Diao).

https://doi.org/10.1016/j.isprsjprs.2023.06.012
Received 22 January 2023; Received in revised form 22 May 2023; Accepted 25 June 2023
Available online 4 July 2023
0924-2716/© 2023 International Society for Photogrammetry and Remote Sensing, Inc. (ISPRS). Published by Elsevier B.V. All rights reserved.

methods, (2) weather-dependent methods, and (3) remote sensing phenological detecting methods. As the most traditional information collection method, field surveys can record accurate crop planting information of individual farm fields. Yet conducting field surveys over wide geographical regions is labor-intensive, time-consuming, and costly. The field collection efforts may also be hampered when the farm fields are private or inaccessible. The weather-dependent methods typically utilize meteorological data around the planting season to estimate the crop planting dates given that weather conditions (e.g., temperature and precipitation suitable for crop germination) are important for farmers' planting decisions (Waha et al., 2012; Waongo et al., 2014; Dobor et al., 2016; Choi et al., 2017; Gümüşçü et al., 2020; Vijaya Kumar et al., 2021). For example, planting usually starts at the onset of the seasonal cycle of temperature when daily average temperature exceeds a certain threshold in the Midwestern US (Choi et al., 2017). The threshold can be determined based on historical temperatures that facilitate the crop planting, and may vary across years, locations, as well as crop types. In addition to setting the specific threshold, potential relationships between crop planting dates and meteorological data can be explored by machine learning techniques (Gümüşçü et al., 2020). The weather-dependent methods show good potential for uncovering coarse crop planting patterns at regional to global scales, but their performance at local scales for farm field planting estimation cannot be guaranteed (Dobor et al., 2016). In addition to weather conditions, crop planting decisions are influenced by several other factors, such as soil conditions, crop species, and availability of machinery.

In recent years, remote sensing has been increasingly utilized to retrieve crop planting dates with its improved resolutions, wide area coverage, and repeated viewing. Due to the intrinsic difficulty in directly capturing the crop planting signal, remote sensing phenological detecting methods have been mainly devised in two types. The first type of remote sensing methods, named phenology matching methods, characterize the crop planting dates of the satellite time series based on a priori crop reference phenological time series and corresponding reference planting dates (Sakamoto et al., 2010; Zeng et al., 2016; Sakamoto 2018; Zhang et al., 2020; Zeng et al., 2020; Diao et al., 2021; Liu et al., 2022). These phenology matching methods (e.g., shape model) align the target satellite time series with the reference phenological time series via geometrical pattern matching. With the aligned relationship, the target planting date can then be estimated by mapping the reference planting date from the reference time series to the target time series. The crop reference phenological time series are pre-defined seasonal crop growth profiles characterized by time series of vegetation indices (VIs), and the reference planting dates are corresponding phenological transition dates of crop planting pre-defined on the reference time series. These crop references are mostly calibrated based on constrained field observations, and have been found to be a major source of uncertainties in crop phenological detection (Diao et al., 2021). The difficulty in formulating appropriate crop phenological reference may limit the ability of phenology matching methods to conduct field-level crop planting estimation.

The second type of the remote sensing phenological detecting methods has mainly focused on retroactively estimating planting dates using the start of season (SOS) metrics identified from the satellite time series (Vyas et al., 2013; Lobell et al., 2013; Phan et al., 2018; Dong et al., 2019; Zhang et al., 2021). The remote sensing SOS metrics can typically be extracted from the time series curves of VIs via threshold-defined algorithms (e.g., 10% or 20% of the curve amplitude) (Chen et al., 2004; Delbart et al., 2006; Zeng et al., 2020) or inflection point algorithms (e.g., local maximum of the rate of curvature change) (Moulin et al., 1997; Schwartz et al., 2002; Zhang et al., 2003; Wu et al., 2017; Gao et al., 2017; Diao, 2020; Diao and Li, 2022). The SOS metrics have been found to approximate the crop vegetative phenological stage after crop emergence, and have time lags for inferring the planting dates (Fig. S1). The time lag between the SOS and the planting date is often assumed unchanged in terms of the number of calendar days or accumulated growing degree days (AGDD) over defined areas and years. Compared to the calendar day-based time lag, the AGDD-based one has been found to perform better with stronger adaptability to different weather conditions by taking into account the thermal time accumulation in the crop growth process (Sacks and Kucharik, 2011; Dong et al., 2019). Despite the important role of AGDD, the time lag between crop planting and SOS metrics involves several crop stages, including germination and emergence. The durations of these stages are affected by a combination of environmental factors (e.g., precipitation and soil conditions) and crop management factors (e.g., planting depth and crop cultivars), and the influence of those factors varies across stages. For instance, the timing of crop germination is mainly affected by the soil moisture content while the crop emergence timing can be affected by both planting depth and soil conditions (Lawlor and Tezara 2009; Way and Yamori 2014). At the farm field level, the SOS-based methods may be subject to biases and errors in estimating crop planting under varying environmental and management conditions. The lack of consideration of the complex soil-crop-atmosphere interactive process underlying crop physiological growth makes the estimation of planting dates challenging, particularly at the field level.

Process-based crop models may potentially help tackle this challenge by simulating field-level crop growth process under combined weather, soil, and management conditions. They integrate mathematical descriptions of the mechanisms affecting the interactive process among crop types, crop management practices, and environment to model crop physiological growth and yield (Asseng et al., 2014; Huang et al., 2019). The widely used crop growth models include Agricultural Production Systems sIMulator (APSIM) (Keating et al., 2003; Holzworth et al., 2014), Decision Support System for Agrotechnology Transfer (DSSAT) (Jones et al., 2003), Multidisciplinary Simulator for Standard Crops (STICS) (Brisson et al., 1998; Brisson et al., 2003), etc. These models encompass comprehensive phenology development schemes with a multitude of stress terms and field management practices to account for the spatiotemporal variation in field-level crop growth and development. During the early season, such rich phenological and physiological information embedded in crop growth models enables the comprehensive simulation of crop phenological phases (e.g., planting to germination, germination to emergence, and emergence to SOS) in response to a range of environmental and management factors, particularly at the field level. Those simulated phenological durations by the crop growth models may thus ease the challenge of the SOS-based planting date estimation methods caused by the insufficient consideration of soil-crop-atmosphere continuum. However, to our knowledge, the potential of crop growth models in retrieving crop planting dates has not been explored.

The overarching goal of this study is to develop an innovative framework, named CropSow, to retrieve the crop planting dates at the field level. CropSow leverages the rich physiological knowledge embedded in the crop growth model to scalably interpret satellite observations under a variety of environmental and anthropogenic conditions for planting date retrievals. With corn in Illinois, US as a case study, the specific aims of our study are threefold: (1) develop CropSow by integrating the remote sensing phenological detecting method with the crop growth model; (2) downscale regional aggregated crop planting information to the field level with rich spatiotemporal planting characteristics; (3) evaluate the CropSow performance upon comparison with three advanced benchmark methods, including the remote sensing AGDD method, the weather-dependent method, and the shape model.

2. Study area and data

2.1. Study area

The study area is the state of Illinois, US, which is one of the largest corn-producing states in the US with its fertile and well-drained soils, as well as warm and humid summers. In Illinois, more than 95% of

croplands are taken up by corn and soybean, and these two major crops are typically rotated in consecutive years. As a rain-fed agricultural area, Illinois experiences various climate conditions across the state, resulting in a variety of corn growth phenological trajectories in different locations and years. Based on climate conditions and cropping practices, nine agricultural statistics districts (ASDs) are defined by the US Department of Agriculture (USDA), namely southwest (SW), southeast (SE), west southwest (WSW), east southeast (ESE), west (W), central (C), east (E), northwest (NW), and northeast (NE) ASDs (Fig. 1).

The study period spans from 2016 to 2020. In 2018, Illinois experienced dramatic temperature swings in the planting season, and had the second coldest April with a mean temperature of 10.7 °C yet the warmest May with a mean temperature of 20.7 °C on record dating back to 1895. In 2019, Illinois had excessive total precipitation of 1053 mm and the second wettest year on record (Li et al., 2019). These unique weather patterns add to the variability in corn phenological development across the state. The diverse corn phenological trajectories and large acreage of corn fields make Illinois a good study site for conducting field-level planting date estimation.

2.2. Data

To date, the most comprehensive and publicly available ground phenological reference data of US are crop progress reports (CPRs), published by the USDA. CPRs provide weekly cumulative percentages of major crops (e.g., corn) that reach certain crop phenological stages. In Illinois, CPRs record corn phenological progress from the end of March to the end of December at the state level from 2016 to 2020. Considering the cumulative corn planting percentage documented in CPRs are widely and openly accessible across US, this regional aggregated crop planting information is utilized to calibrate the CropSow framework. As for the satellite data, we acquire the Moderate Resolution Imaging Spectroradiometer (MODIS) MCD43A4 imagery for conducting the framework calibration. With the calibrated CropSow, we then utilize the Harmonized Landsat 8 and Sentinel-2 (HLS) imagery for estimating crop planting dates at the farm field level. During the process of framework calibration and field planting date estimation, the normalized difference vegetation index (NDVI), as the most widely used vegetation index for measuring crop growth conditions, is employed for crop phenology monitoring (Seo et al., 2019).

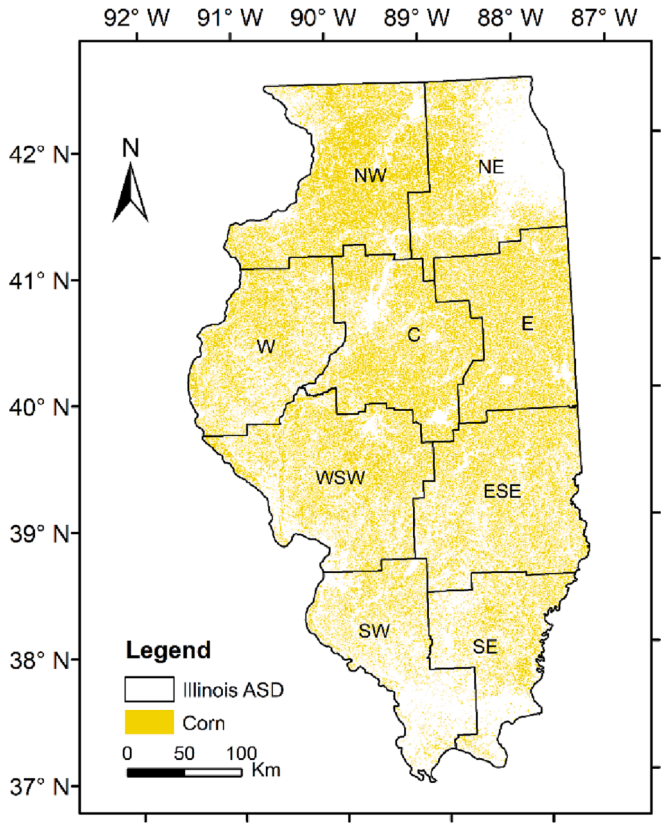

Fig. 1. Illinois agricultural statistics district (ASD) boundary and corn fields (2020).

We acquire the MODIS MCD43A4 (version 6) nadir Bidirectional Reflectance Distribution Function (BRDF) adjusted reflectance product with daily temporal resolution and 500 m spatial resolution for calibrating the CropSow at the state level. The combination of spatial and temporal resolutions of MODIS is an adequate tradeoff for the state-level framework calibration. In particular, the MODIS daily observation frequency facilitates the detection of subtle changes around crop planting dates during the early growing season. The 500 m spatial resolution can help locate an adequate number of pure pixels of corn fields across Illinois while maintaining the computational efficiency of the framework calibration. Specifically, we utilize the yearly Cropland Data Layer (CDL) data to select pure corn MODIS pixels. The CDL is a raster formatted crop-specific land cover map with a spatial resolution of 30 m, produced by the USDA (Boryan et al., 2011). It has been updated annually for various crop types (e.g., corn and soybean) over the Conterminous United States (CONUS) since 2008. The CDL products are highly accurate on corn and soybean classes (generally over 95% producer's and user's accuracies) (Sun et al., 2020), and are publicly available from CropScape (https://nassgeodata.gmu.edu/CropScape/). The pure corn MODIS pixels are identified as the pixels with the percentage of corn higher than 90% based on CDLs. In total, there are 30566, 26939, 24841, 23975, and 28,510 pure corn pixels for the years 2016, 2017, 2018, 2019, and 2020, respectively. The CropSow framework is annually calibrated using the corresponding CPR based on the MODIS generated NDVI time series of all pure corn pixels in Illinois.

With the calibrated CropSow framework, we then acquire the HLS Version 1.5 dataset for estimating corn planting dates of individual farm fields. The HLS dataset provides radiometrically consistent surface reflectance imagery from Landsat 8, Sentinel-2A, and Sentinel-2B satellites. This harmonized product is generated through atmospheric correction and cloud masking, spatial co-registration, BRDF normalization, band pass adjustment, and temporal compositing. The harmonization of three satellites' images can achieve a temporal resolution of every 2–3 days and a spatial resolution of 30 m (Li and Roy 2017). Because of the late launch of Sentinel-2B satellite in 2017, the HLS images before 2017 are only generated from Landsat 8 and Sentinel-2A, and the temporal resolution of HLS images is relatively lower in the first year of our study period (2016) than that in the following years. The HLS images may also be subject to the influence of cloud, cloud shadow, and haze, resulting in varying numbers of high-quality images across locations and years. The HLS images are thus not directly utilized for the framework calibration but represent a good tradeoff for flexibly retrieving the phenological characteristics of individual corn fields in Illinois. The boundaries of Illinois corn fields are obtained from the Common Land Unit (CLU) dataset and corresponding CDLs. The CLU dataset, produced by the USDA, provides contiguous boundaries of the smallest unit of agricultural land. Within each individual corn field, high-quality pixels are selected from all available HLS images based on their corresponding quality assessment (QA) layers to eliminate the negative effects of cloud and haze. NDVI values of all selected pixels within the same cropland are averaged on a day-to-day basis each year to generate annual field-level NDVI time series for that targeted cropland.

For the crop growth model of the CropSow framework, we obtain the data of essential model inputs regarding the soil and meteorological conditions. The soil inputs, such as layered soil hydraulic properties, soil pH, and soil organic matter, are queried from the Gridded Soil Survey Geographic (gSSURGO) dataset. The gSSURGO dataset is a 30 m spatial

soil raster map derived from the vector-based Soil Survey Geographic (SSURGO) database, in which many soil samples have been collected by the National Cooperative Soil Survey and further analyzed in laboratories for the database construction. The daily meteorological inputs include daily minimum and maximum temperatures, precipitation, vapor pressure, shortwave radiation, snow water equivalent, and day length (Thornton et al., 2016). They are derived from the Daymet dataset, which is a long-term, continuous, 1 km × 1 km gridded dataset of daily meteorological variables over continental North America and Hawaii from 1980 to the end of the most recent full calendar year. With the soil and meteorological inputs, the crop growth model is utilized to simulate the corn phenological development from planting to following vegetative stages in CropSow.

To validate the performance of CropSow, we also collect field-level corn planting date data from Beck's Hybrids (publicly accessible via https://www.beckshybrids.com/Research/Yield-Data), with a total of 379 field planting date samples from 2016 to 2020. The fields are distributed across nine ASDs of Illinois with an average size of around 0.4 km^2. The annual number of the collected corn field planting date records within each ASD is shown in Fig. 2. The number of corn planting records varies across ASDs and years, and in general the central ASD has more planting records than other ASDs. Given the difficulty in obtaining the field-level crop planting information at large scales, this dataset is only used for CropSow validation, but not for calibration.

3. Methodology

The CropSow framework mainly consists of two key components: remote sensing phenological detecting method and crop growth model (Fig. 3). The remote sensing phenological detecting method encompasses time series phenological pre-processing, time series phenological fitting, and time series phenological characterization to extract the SOS phenological metrics from remote sensing image series. The crop growth model is utilized to estimate the time lag between the actual crop planting date and remote sensing SOS phenological metrics with consideration of soil-crop-atmosphere continuum. The crop growth model is calibrated through the MODIS time series and CPR-documented planting dates at the state level. With the calibrated CropSow, we then employ the HLS time series to estimate the crop planting dates at the field level. The CropSow's performance is further assessed in comparison with three advanced benchmark methods, namely the remote sensing AGDD method, the shape model, and the weather-dependent method.

3.1. CropSow

3.1.1. Remote sensing phenological detecting method

The remote sensing phenological detecting method is developed to obtain the SOS phenological metrics with three main modules: time series phenological pre-processing, time series phenological fitting, and time series phenological characterization.

Time series phenological pre-processing consists of two main steps, namely removal of outlier observations and removal of off-season peaks. Due to the influence of cloud and haze on remote sensing imagery, there exist spurious or implausible outliers that could potentially affect the subsequent phenological fitting processes. The first step utilizes a set of filtering algorithms (i.e., night filter, spline filter, and mad filter) sequentially to filter out those contaminated observations in the NDVI time series (Fig. S2). The night filter is employed to remove observations of low NDVI values that are typically caused by low illumination conditions, cloud, and snow. The NDVI values that are abnormally lower than the median off-season NDVI values are removed with this filter. The spline filter proposed by Migliavacca et al. (2011) is a cubic smoothing spline filter that suppresses unusually high or low observation values. To filter out the unusual values, a smoothing spline is first fitted based on original NDVI time series. Residuals are obtained by calculating the difference between the daily NDVI values and corresponding smoothing spline fitted values. The mean (μ) and standard deviation (σ) of the residuals are then derived, and unusual values are defined as the observations with the absolute value of residuals larger than $\mu + 3\sigma$. Those unusual values are removed recursively until no unusual observations are detected. The mad filter, following the method of Papale et al. (2006), is applied to remove spikes on the NDVI time series according to the median absolute deviation (MAD). MAD is a robust measure of how spreading out a set of data is. The NDVI values that cause large MAD are identified as spikes, which are then removed to improve the quality of NDVI time series. The gaps of outlier-removed NDVI time series are filled via linear interpolation.

Apart from outliers, the remote sensing time series may contain off-season plant growing cycles which are unrelated to the target crop species. Such off-season growing cycles are usually caused by weeds, cover crops, or double crops, and may affect the characterization of phenological metrics of the target crop. Therefore, the second step is to use a seasonality filter to further smooth out off-season growing cycles, so that only targeted growing cycles are retained (Fig. S2). Specifically, the seasonality filter employs a smoothing spline algorithm to capture the general dynamic patterns of plant growth using the outlier-removed NDVI time series. The turning points (i.e., peaks and pits) of the spline

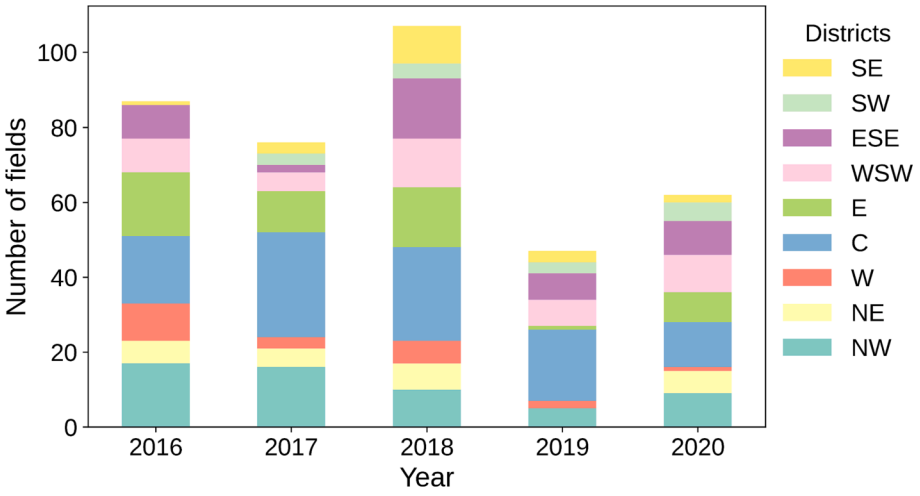

Fig. 2. Number of ground reference corn field planting date records of Illinois by agricultural statistics district (ASD) and year. Nine ASDs in Illinois are southwest (SW), southeast (SE), west southwest (WSW), east southeast (ESE), west (W), central (C), east (E), northwest (NW), and northeast (NE) ASDs.

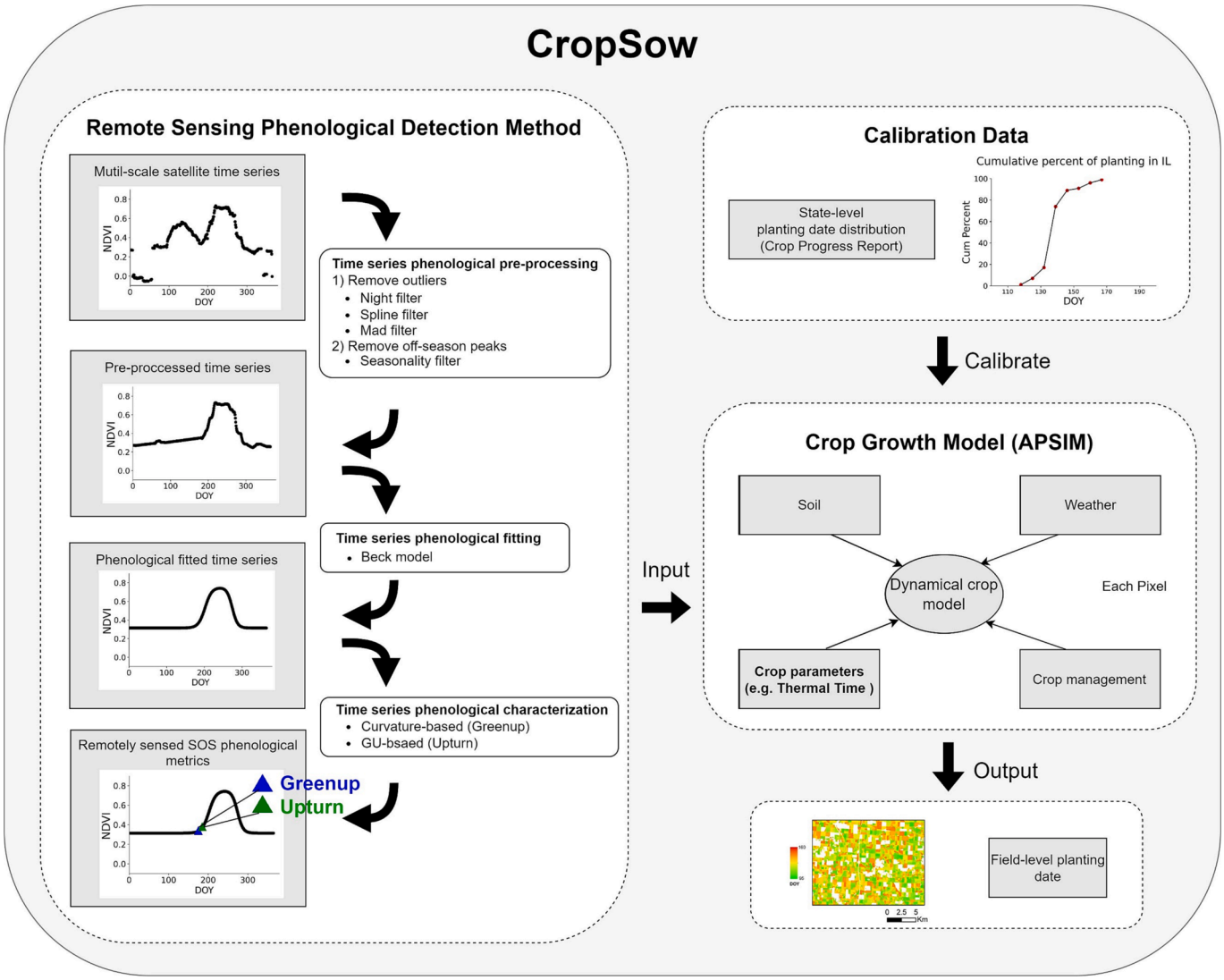

Fig. 3. Flowchart of CropSow for field-level crop planting date estimation.

smoothed curve are utilized to identify the growing cycle of the target crop species in consideration of corresponding peak NDVI values and crop calendars from CPRs. Specifically, the peak NDVI timing of the target growing cycle is constrained to be within the period from three weeks ahead of the start of corn silking stage to the start of maturity stage of CPRs. The other cycles with localized peaks during the off-season of the target crop are then removed.

After time series phenological pre-processing, the phenological growing profile of the target crop is obtained through time series phenological fitting using the Beck's double logistic method. Compared to other time series phenological fitting methods (e.g., asymmetric Gaussian fitting method, Savitzky–Golay fitting method, quadratic fitting method, and nonlinear spherical fitting method), the double logistic fitting method can better characterize the phenological profiles of vegetation with rapid phenological transitions and relatively short growing seasons, without overestimating the growing season durations (Beck et al., 2006). It is thus employed in this study to detect crop phenological dynamic changes at the beginning of the growing season. Specifically, the Beck's method fits the pre-processed NDVI time series using a generalized double logistic function with six parameters to model crop phenological development (Eq. (1)).

$$f(t) = V_{base} + (V_{max} - V_{base}) * \left(\frac{1}{1 + e^{(-m_1 * (t - m_2))}} + \frac{1}{1 + e^{(-n_1 * (t - n_2))}} - 1 \right) \quad (1)$$

where t is the day of year (DOY) and $f(t)$ is the corresponding fitted NDVI value. V_{base} is the off-season NDVI value, and V_{max} is the maximum NDVI value over the course of a year. m_2 and n_2 denote the timing of inflection points of the curve rising and dropping, respectively. m_1 and n_1 correspond to the rates of curve change at those two points (m_2 and n_2), respectively. The six parameters are estimated via the least square method which minimizes the root mean square errors (RMSEs) between $f(t)$ and the pre-processed NDVI time series.

Lastly, the SOS phenological metrics are extracted from the Beck fitted NDVI time series via time series phenological characterization. Both threshold-based methods and inflection point methods can be used for phenological characterization. Compared to threshold-based methods, inflection point methods can more robustly and effectively extract phenological metrics for various crop types in different locations based on the curvature change characteristics of NDVI time series, without customizing cultivar- and location-specific thresholds (Zeng et al., 2020; Diao 2020). In this study, two inflection point methods, the curvature-based method and the GU-based method, are leveraged to retrieve the SOS phenological metrics (Fig. 4), as these two methods have been demonstrated to approximate the initial corn vegetative stage (e.g., corn V3 stage with about 2–4 leaves) (Gao et al., 2017; Diao 2020). The curvature-based method characterizes the SOS when the change rate of curvature of the fitted NDVI time series reaches its first local

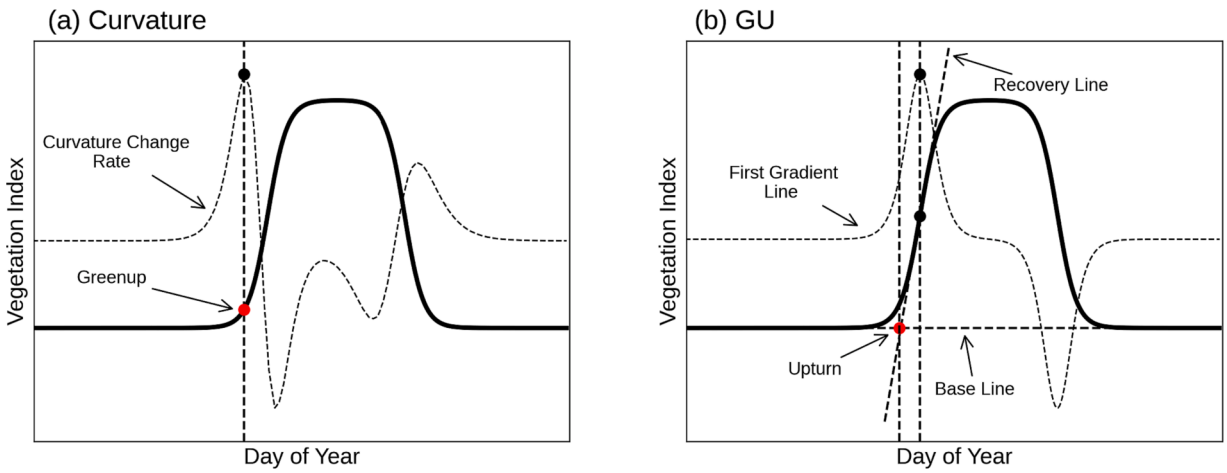

Fig. 4. Schematic of SOS metric extraction using curvature-based method (a) and GU-based method (b).

maximum, and this curvature-derived SOS is termed as Greenup (Beck et al., 2006). The GU-based method characterizes the SOS as the time of intersection between the recovery line and base line of the fitted NDVI time series curve (Gu et al., 2009). The base line is defined as the horizontal line at the minimum value of the fitted NDVI time series curve. The recovery line is defined as the tangent line to the fitted NDVI time series curve at the curve point with the maximum first derivative. The GU-derived SOS is termed as Upturn in this study. The curvature-derived Greenup and GU-derived Upturn SOS metrics will be utilized in the subsequent crop growth model.

In this study, the above procedures are leveraged to extract the SOS phenological metrics from both MODIS and HLS time series, with the MODIS metrics further used for crop model calibration and the HLS metrics used for field-level planting date estimation.

3.1.2. Crop growth model (APSIM)

Plant growth and development mainly depend on the interactions among crop types, crop management, and environment. Crop growth models take into account a variety of interactive processes underlying the soil-crop-atmosphere continuum to simulate crop phenological development. Hence, crop growth models have great potential in scalably and effectively estimating the duration between crop planting and following stages under varying weather conditions and crop management practices. APSIM, as one of widely used crop growth models in predicting corn phenological timing in the midwestern US, is utilized to estimate the time lag between the corn planting date and remote sensing SOS phenological metrics.

After the planting of corn seed, corn experiences germination and emergence stages, and then reaches the SOS phenological metrics that are around the V3 stage. In APSIM, the commencement of the germination is driven by soil water status. After the germination stage, the corn phenological development is driven by temperature accumulation termed as daily thermal time accumulation (in degree days). APSIM determines the duration of phenological phases by taking into account the speed and requirement of temperature accumulation. Factors such as water and nitrogen stress can impact the speed of temperature accumulation, and the thermal time requirement may vary depending on crop management practices and phenological stages. For example, the thermal time requirement from corn germination to emergence is mainly determined by the planting depth, as the seedling emergence is the process encompassing the plumule growth towards the soil surface and coming out from the soil. The thermal time requirement from emergence to the following vegetative stage is mainly determined by the number of corn-collared leaves and the thermal time requirement for the development of a leaf, namely *phyllochron*. The *phyllochron* is relatively comparable among various corn cultivars (Birch et al., 1998; Dos Santos et al., 2022; Morel et al., 2020; Plancade et al., 2022). Given the SOS metrics approaching the corn V3 stage (i.e., three collared leaves), the thermal time requirement from the emergence stage to remote sensing SOS metrics can also be assumed to be comparable across cultivars, and is defined as *tt_emerg_to_sos* in degree days.

In APSIM, many modules are designed to simulate crop phenological progress, including the SoilWater module, the SoilNitrogen module, and the Phenology module. Each day, the SoilWater module calculates the daily soil moisture based on soil physical and weather conditions. Seeds germinate when the soil moisture is appropriate for the initiation of seed sprouting. The Phenology module calculates the daily thermal time using 3-hourly air temperatures interpolated from the daily minimum and maximum temperatures. The SoilWater and the SoilNitrogen modules can also simulate the effects of soil water deficit and soil nitrogen deficit on the crop growth, respectively. The daily thermal time will be adjusted according to the water and nitrogen stresses calculated by these modules. The daily thermal time values are then accumulated into a thermal time sum to determine the duration between each two crop phenological stages. In this study, the thermal time sum *tt_emerg_to_sos* is calibrated using the state-level CPRs as well as pure MODIS pixels of Illinois to retrieve the duration from the corn emergence stage to remote sensing SOS metrics. The APSIM input variables (except planting dates) are set in reference to previous studies conducted for corn in the Midwestern US (Table 1) (Mandrini et al., 2022). A range of corn planting dates (i.e., April 1 – June 1) are attempted for the calibration of *tt_emerg_to_sos* upon comparison to CPRs.

Specifically, the calibration of thermal time sum *tt_emerg_to_sos* is shown in Fig. 5. Firstly, for each pure MODIS pixel, APSIM initially runs with the planting date of April 1 and the *tt_emerg_to_sos* of 0 ℃-day, as well as the soil, weather, and other crop management inputs (Table 1) to derive the model estimated SOS. If the model estimated SOS does not match with the MODIS pixel's remote sensing SOS phenological metric, the planting date input is added by one day. The APSIM iteratively runs with an updated planting date until the model estimated SOS aligns with the pixel SOS phenological metric, and the updated planting date of this alignment is regarded as the model estimated planting date for this pixel. Under the condition of *tt_emerg_to_sos* being 0 ℃-day, all pure corn MODIS pixels' planting dates are then estimated and utilized to generate temporal cumulative distribution of model estimated planting dates at the state level. This temporal cumulative distribution is compared to that of actual planting dates from CPRs. The degree of similarity is quantified by the RMSE between the cumulative planting percentages of CPRs and those of model estimation. By minimizing the RMSE, the optimal *tt_emerg_to_sos* can then be estimated from a range of 0–300 ℃-day for the parameter calibration. Given the SOS phenological metrics derived from MODIS along with the complicated soil-crop-

Table 1
Input variables for APSIM simulations.

Variable	Value	Description	Reference
Fertilizer	160 kg/ha (Default)	Amount of fertilizer	Default in APSIM
Initial nitrogen	40 kg/ha	Amount of Initial nitrogen	(Mandrini et al., 2022)
Planting dates	April 1 – June 1	Date when crop is planted	CPRs
Initial water	50%	Amount of initial water on the first day of that year	Default in APSIM
Soil pH	gSSURGO	A measure of soil acidity or alkalinity	USDA-NASS
Soil hydraulic properties	gSSURGO	The hydraulic properties of the soil (infiltration, hydraulic conductivity, water retention, and available water capacity)	USDA-NASS
Soil organic matter	gSSURGO	The fraction of the soil that consists of plant or animal tissue in various stages of breakdown (decomposition)	USDA-NASS
Weather	DAYMET	Daily minimum and maximum temperature, precipitation, vapor pressure, shortwave radiation, snow water equivalent, and day length	(Thornton et al., 2022)
Initial surface residue	2000 kg/ha of soybean	Amount of initial residue from previous crop	(Mandrini et al., 2022)
Planting density	9 plants/m^2	Density of maize seed being sown	(Mandrini et al., 2022)
Planting depth	50 mm	Depth of maize seed being sown	(Mandrini et al., 2022)
Row spacing	760 mm	Spacing between rows	(Baum et al., 2020)

atmosphere interactive process simulated by APSIM, the *tt_emerg_to_sos* is calibrated on a yearly basis using the corresponding year-specific CPR.

With the *tt_emerg_to_sos* parameter calibrated, APSIM can simulate the crop phenological development in the early season and estimate the number of days from corn planting to HLS-derived SOS phenological metrics of individual farm fields. The field-level corn planting dates can thus be estimated with the integration of remote sensing phenological detecting method and the calibrated APSIM model.

3.2. Benchmark methods

This section introduces three advanced benchmark methods for crop planting date estimation. The benchmark methods include the remote sensing AGDD method, the shape model, and the weather-dependent method. Similar to CropSow, the three benchmark methods are calibrated using the MODIS time series and CPR-documented planting dates at the state level. After the method calibration, the HLS time series is employed to estimate corn planting dates at the farm field level.

3.2.1. Remote sensing AGDD method

As a major SOS-based remote sensing phenological detecting method, the remote sensing AGDD method estimates the crop planting date retroactively using the remote sensing SOS metric and the AGDD-based time lag (Dong et al., 2019). The time lag from the crop planting date to the SOS date can usually be represented using the number of calendar days or AGDD. Compared to the calendar day-based time lag, the AGDD-based one has been found to perform better with stronger adaptability to different weather conditions by taking into account the thermal time accumulation in the crop growth process, and is thus utilized in this study. The planting date can then be estimated by subtracting the AGDD-based time lag from the remote sensing SOS metric. In this study, the remote sensing SOS metric is the Greenup metric retrieved from the NDVI time series using the curvature-based method, similar to the Greenup metric in CropSow. The AGDD-based time lag is calibrated on a yearly basis using the MODIS time series and the corresponding year-specific CPR. Specifically, the AGDD from the planting to the SOS dates is optimized each year to minimize the RMSE between the estimated temporal cumulative distribution of planting dates of the pure corn MODIS pixels and the corresponding reference cumulative distribution of corn planting dates in CPRs at the state level. As a measure of heat accumulation to quantify plant development rates, the daily growing degree day (GDD) is calculated using the daily maximum temperature (T_{max}), the daily minimum temperature (T_{min}), the daily base temperature (T_{base}), and the daily capped maximum temperature (T_{cap}) (Eq. (3)). In Illinois, the T_{base} is usually set as 10 °C and the T_{cap} is typically set as 30 °C for corn (Wang, Azzari, and Lobell 2019).The corresponding AGDD is then calculated by summing up the daily GDD from the planting date to the SOS date (Eq. (2)). With the annual calibrated AGDD ($AGDD_{sos}$), the planting dates of individual farm fields could be estimated using the curvature-derived Greenup SOS metrics from the HLS time series (Eq. (4)).

$$AGDD_{sos} = \sum_{doy=planting\ date}^{SOS} GDD_{doy} \tag{2}$$

$$GDD_{doy} = \max\left(\frac{min(T_{max}, T_{cap}) + max(T_{min}, T_{base})}{2} - T_{base}, 0\right) \tag{3}$$

$$Planting\ date = SOS - days(AGDD_{sos}) \tag{4}$$

3.2.2. Shape model

As a benchmark phenology matching method, the shape model is designed to estimate crop phenological transition dates (e.g., planting dates) through matching the geometrical patterns of the target and reference phenological time series (Sakamoto et al., 2010; Sakamoto 2018; Liu et al., 2022) (Fig. 6). The target phenological time series is the NDVI time series of the target pixel for planting date estimation, and the reference phenological time series is the corn-specific NDVI time series curve defined as the 90th percentile of all the pure corn MODIS pixels' NDVI curves on a yearly basis in reference to our previous study (Diao et al., 2021). The shape model assumes that the target phenological time series can be geometrically matched through the scaling and shifting of the reference phenological time series. With the geometrically matched relationship, the target planting date can be estimated by mapping the reference planting date from the reference phenological time series to the target phenological time series (Fig. 6). In this study, we calibrate the reference planting date on a yearly basis by searching all the dates within the range of two weeks before and after the median date of the corn planting in the corresponding CPRs. The reference planting date is calibrated as the date that leads to the lowest RMSE between the temporal cumulative distribution of corn planting dates from the CPRs and that of the planting dates of the pure corn MODIS pixels estimated by the shape model. With the calibrated reference planting date and predefined reference phenological time series, the shape model is then employed to estimate the planting dates of target farm fields using the HLS NDVI time series curves.

The geometrical matching process of the shape model is defined in Eq. (5).

$$f(DOY) = VI_{scale} \times r(DOY_{scale} \times (DOY + DOY_{shift})) \tag{5}$$

where the function *r(DOY)* represents the NDVI value of the reference phenological time series on a certain *DOY*, and *f(DOY)* refers to the NDVI value of the fitted phenological curve on the *DOY*. VI_{scale} and DOY_{scale} denote the magnitude of scaling of the reference phenological curve on the vertical and horizontal axes, respectively. DOY_{shift} denotes the relative shift of phenological timing on the reference phenological curve.

The optimum scaling parameters (e.g., VI_{scale}, DOY_{scale}, *and* DOY_{shift}) are determined by minimizing the RMSE between the fitted phenological curve *f(DOY)* and the target phenological curve *t(DOY)* (Eq. (6)).

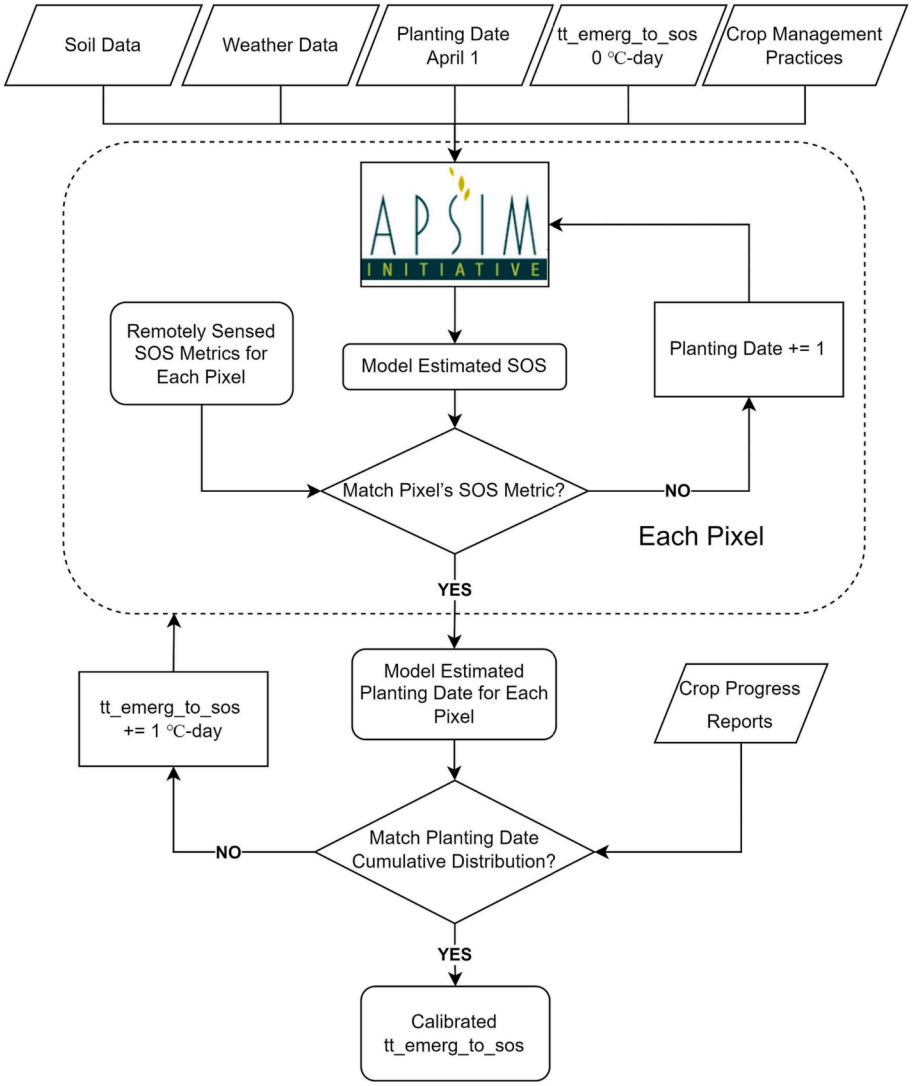

Fig. 5. Workflow of the APSIM parameter calibration.

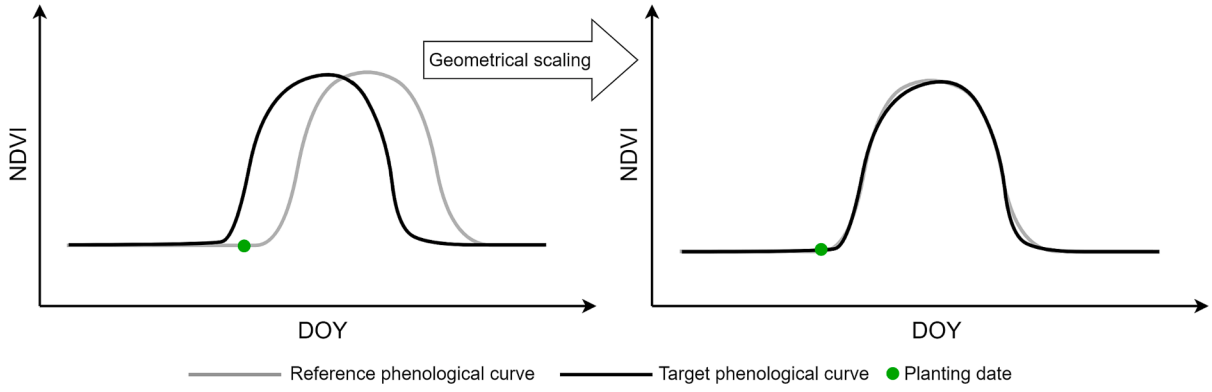

Fig. 6. Schematic of geometric matching between reference and target phenological time series curves using the shape model.

The search ranges for these three parameters are empirically set as follows: $0.3 < DOY_{scale} < 1.5$, $0.3 < VI_{scale} < 1.5$, and $-80 < DOY_{shift} < 80$ (Sakamoto et al., 2010).

$$RMSE = \sqrt{\frac{1}{73}\sum_{DOY=5,10,15\cdots}^{365}(f(DOY) - t(DOY))^2} \quad (6)$$

With the calibrated reference phenological planting date and the optimum scaling parameters specifically fitted for each target phenological curve, the planting date on the target phenological curve is estimated through the geometric transformation equation (Eq. (7)).

$$PD_t = \frac{1}{DOY_{scale}^{opt}} \times PD_r - DOY_{shift}^{opt} \quad (7)$$

where PD_t is the estimated planting date on the target phenological curve, and PD_r is the calibrated reference planting date on the reference phenological curve. DOY_{scale}^{opt} and DOY_{shift}^{opt} are the optimum scaling parameters.

3.2.3. Weather-dependent method

The weather-dependent methods typically utilize the meteorological data to estimate the crop planting dates, given that the weather conditions (e.g., temperature and precipitation) suitable for crop germination are important for farmers' planting decisions. For example, too much rain can saturate the soil, causing poor soil aeration, poor germination, and poor stands. Too little rain may dry out the soils in rainfed areas, causing weak and small plants that may not withstand the weather over the subsequent growth stages (Heng et al., 2009). Lower or higher temperature can slow down the seed germination process (Covell et al., 1986).

In this study, the weather-dependent method employs a set of rules in consideration of the critical meteorological and environmental factors influencing the corn seed germination to estimate the planting dates (Dobor et al., 2016). With reference to previous studies and extension research in Illinois, the critical factors encompass the air temperature, soil temperature, and normalized water content (NWC). The rules for estimating the corn planting dates include: (1) the average air temperature is larger than t_1 °C for five consecutive days before the planting dates, (2) the temperature of the topsoil from 0 to 15 cm is larger than t_2 °C for five consecutive days before the planting dates, and (3) the NWC of the planting date is within the 20–80% range. The satellite data are not used in the weather-dependent method. The temperature parameters, t_1 and t_2, are calibrated on a yearly basis through minimizing the RMSE between the annual temporal cumulative distribution of corn planting dates from the CPRs and that of the planting dates of the pure corn MODIS pixels estimated by the rules of the weather-dependent method. The NWC is defined as:

$$NWC = 100 \times \frac{\theta - \theta_r}{\theta_s - \theta_r} \tag{8}$$

where θ is the volumetric water content. θ_r and θ_s are the residual and the saturated water content of the soil, respectively. Due to the lack of data on volumetric water content, θ is calculated via the SoilWater module of APSIM. θ_r and θ_s are retrieved from the gSSURGO dataset.

3.3. Framework evaluation

CropSow's and other three benchmark methods' corn field planting date estimations are directly compared with the reference field-level planting dates from the Beck's dataset. The coefficient of determination (R^2), the mean bias error (MBE), and the RMSE are calculated to assess the accuracy of the estimated planting dates. The R^2 measures the proportion of the variance in the observed planting dates explained by the corresponding estimated planting dates. The RMSE and MBE both measure the errors of the estimations. Specifically, the MBE captures the average bias in the estimation and the RMSE describes how close the observed planting dates are to the estimated ones. The RMSE, MBE and R^2 are calculated using the Eqs. (9)–(11), respectively. The spatial–temporal patterns of those accuracy measures across ASDs and years are further investigated. Given the varying number and quality of HLS images across locations and years, the influence of HLS image availability on the planting date estimation performance is also evaluated.

$$RMSE = \sqrt{\frac{1}{N}\sum_{i=1}^{n}(P_i - O_i)^2} \tag{9}$$

$$MBE = \frac{1}{N}\sum_{i=1}^{n}(P_i - O_i) \tag{10}$$

$$R^2 = \frac{\sum_{i=1}^{n}(P_i - \overline{P})^2}{\sum_{i=1}^{n}(O_i - \overline{P})^2} \tag{11}$$

where P_i is the estimated planting date and O_i is the observed plating date of the sample i. N denotes the number of samples; $\overline{P}$ denotes the mean value of all observed planting dates.

As crop management input data might not always be available over large scales, we conduct a global sensitivity analysis to explore how model performance is affected by several input management variables (e.g., fertilizer, initial water, planting density, and planting depth) and our selected phenological parameter (i.e., *tt_emerg_to_sos*) for calibration. This sensitivity analysis is conducted using the Extended Fourier Amplitude Sensitivity Test (EFAST) method, with the range of each variable (or parameter) set according to literatures for the US corn management practices (Table S1) (Westgate et al., 1997; Mandrini et al., 2022; Nemergut et al., 2021). EFAST employs a multi-phase Fourier series decomposition method to decompose the variance of the model output into partial variances associated with each variable (or parameter). It enables the estimation of total and main effects of a variable (or parameter) by analyzing its contributions to the output variance. Total effect measures the overall impact of a tested variable (or parameter), including both its direct impact and the impact from its interactions with other variables (or parameters), while main effect measures the direct impact of an input variable (or parameter) on CropSow's performance without considering the interaction effect. The performance of CropSow is evaluated via the comparison between the cumulative percentage distribution of estimated planting dates under different combinations of these five variables (or parameters) with corresponding reference cumulative distribution of planting dates from CPRs using RMSE.

To further evaluate the CropSow performance at the ASD level, we compare the temporal cumulative distribution of estimated corn planting dates with that of CPR-documented planting dates for each ASD of Illinois. Specifically, within each ASD, we randomly select 200 corn fields using the CLU and CDL in consideration of both sample size and computational cost, and estimate the corresponding planting dates using CropSow. The temporal cumulative distribution of the estimated planting dates is then generated for the ASD-level framework evaluation. Since the ASD-level CPRs are not publicly available after 2017, the ASD-level framework evaluation is implemented in 2016 and 2017.

With the ASD-level CPRs in 2016 and 2017, we further calibrate the CropSow at the ASD level for these two years to evaluate the influence of the spatial aggregation level of CPRs on the framework performance. For each ASD and year combination, CropSow is calibrated using the corresponding cumulative corn planting information in CPRs. We then compare the performance of CropSow calibrated at the ASD level with that of CropSow calibrated at the state level using the Beck's dataset.

To evaluate the generalizability of the CropSow framework, we also estimate the field-level planting dates for one year (the target year) using the state-level CropSow framework calibrated with other years data. Specifically, for a target year, CropSow is calibrated with each of the other four years' data, respectively. With the calibrated CropSow, the field-level planting dates of the target year can then be estimated and evaluated using the Beck's data in terms of the accuracy metrics (RMSE, MBE and R^2). For each accuracy metric, the average of the metric values of four calibrations for the target year is calculated to assess the generalizability of CropSow being calibrated using non-target years' data. The generalizability of the benchmark methods is evaluated in the same fashion. We further generate the corn field planting date maps of the Champaign and Dekalb counties of Illinois from 2016 to 2020 using CropSow. The Champaign and Dekalb counties are located in central and northern Illinois, respectively. These two counties are under different weather conditions, with corn fields exhibiting various phenological trajectories. All the corn fields of these two counties are located using the CLU and CDL, and the planting dates of corn fields are estimated accordingly using CropSow. The spatio-temporal planting

date patterns of corn fields are then investigated and compared for these two counties to evaluate the framework.

4. Results

4.1. Temporal cumulative distribution of crop phenology

In Illinois, field planting progress for corn was surveyed and reported in the CPRs. From 2016 to 2020, the annual temporal cumulative distribution of planted corn fields in Illinois is shown in Fig. 7. The cumulative distribution curve of planted fields differs year by year. The planting windows in 2016, 2017, and 2020 are relatively comparable, mostly ranging from DOY 100 to DOY 160. The planting windows in 2018 and 2019 are more disparate compared to the three other years. In 2018, the planting practice happened mainly within a narrow window from DOY 110 to DOY 140, whereas it happened within an extremely wide window from DOY 110 to DOY 180 in 2019. The variability of planting progress is partly due to the various planting decisions made by farmers under different weather conditions (e.g., dramatic temperature swings may facilitate the corn planting in 2018; excessive precipitation may delay the corn planting in 2019).

CropSow framework is calibrated with the temporal cumulative distribution of the remote sensing SOS metrics (e.g., Greenup or Upturn) extracted from pre-processed MODIS time series and that of planted fields from CPRs. Fig. 8 displays the annual temporal cumulative distribution of actual planted fields and emerged fields from CPRs (solid red and green lines), Greenup and Upturn metrics extracted from MODIS time series (solid blue and yellow lines), and planting dates estimated by calibrated CropSow based on Greenup or Upturn (dashed blue and yellow lines) in Illinois from 2016 to 2020. The temporal cumulative distributions of planting dates estimated by calibrated CropSow (Greenup or Upturn) are well matched with those of actual planted fields from CPRs, demonstrating the validity of calibration of CropSow at the state level. In contrast, both of the two remote sensing SOS metrics' curves tend to be closer to the CPR emerged curve instead of the CPR planted curve. The remote sensing signals of SOS metrics are generally detected 3–4 weeks after planting, except for 2019 when the excessive precipitation conditions complicate the remote sensing characterization of the SOS metrics. The early-season weed growth and delayed corn planting in 2019 changes the pattern of remote sensing time series and the distribution of SOS metrics. It is also noted that the temporal cumulative distribution curves of the Greenup metrics are around 3 days earlier than those of the Upturn metrics across all five years.

4.2. Field-level planting date estimation

Under the calibrated CropSow framework, field-level planting dates are estimated in Illinois from 2016 to 2020 through phenological metrics extracted from the HLS satellite time series and the physiological knowledge embedded in the APSIM. We assess the performance of the CropSow framework in estimating field-level planting dates in different years and spatial levels (i.e., state level and ASD level). We then explore the potential of improving the framework's planting date estimation performance by calibrating the framework with ASD-level CPRs data available in 2016 and 2017.

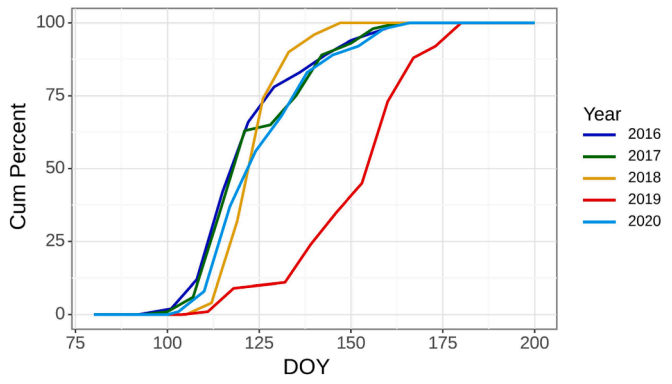

Fig. 7. Annual temporal cumulative distribution of planted corn fields from CPRs in Illinois from 2016 to 2020.

4.2.1. CropSow performance

Fig. 9 shows the scatterplots of the planting dates estimated by annual calibrated CropSow (Greenup) or CropSow (Upturn) against the corresponding actual field-level planting dates in the Beck's dataset from 2016 to 2020. Each point represents a record of an agricultural field in Beck's dataset. In general, the data points in both scatterplots are close to the 1:1 line (solid diagonal line), with most points falling within the ±10 days boundaries (dashed lines). The distribution of the data points suggests the satisfactory performance of CropSow in estimating field-level planting dates. Compared to CropSow (Upturn), CropSow (Greenup) shows better performance in field-level planting date estimation with higher R^2 (0.69 vs. 0.59), lower MBE (5.07 vs. 6.62 days), and lower RMSE (9.13 vs. 11.75 days). The scatterplots also suggest that the estimation bias (e.g., the fields with actual planting dates around DOY 110) is much smaller when CropSow (Greenup) is employed. Pairwise *t*-test is conducted to further test the difference between the estimations generated by the two SOS metrics, and the result ($p < 0.01$) reconfirms that CropSow (Greenup) exhibits significantly better performance compared to CropSow (Upturn). The good results demonstrate the applicability and validity of downscaling regional aggregated crop planting information to the field level through the integration of remote sensing observations and APSIM.

Fig. 10 shows the yearly scatterplots of estimated planting dates against the Beck's actual planting dates, using CropSow (Greenup) or CropSow (Upturn). Significant positive correlations are observed between the estimated and actual planting dates in all combinations of years and SOS metrics, ranging from 0.52 to 0.91 (R^2 between 0.27 and 0.84). Overall, CropSow (Greenup) tends to yield higher R^2, and lower RMSE and MBE compared to CropSow (Upturn). In 2016, 2017 and 2019, CropSow (Upturn) substantially overestimates the planting dates, leading to a larger number of points skewed to the left of 1:1 line and falling out of the ±10 days boundaries. In contrast, the estimation results of CropSow (Greenup) are closer to the diagonal 1:1 line. In 2018, data points are densely distributed in a narrow window for both two metrics, likely due to early planting caused by the warm spring in that year. In 2020, the two metrics achieve satisfactory estimation results, both with R^2 over 0.8 and MBE lower than 3 days. In terms of quantitative measures, CropSow (Greenup) generates lower RMSE values compared to CropSow (Upturn) in all the five years. CropSow (Greenup) also gives substantially higher R^2 from 2016 to 2018, and the two SOS metrics generate almost the same R^2 values in 2019 and 2020. As for MBE, CropSow (Greenup) demonstrates significantly better performance in 2016 (6.7 vs. 11.11 days) and 2019 (7.74 vs. 12.04 days), while the two SOS metrics generate comparable MBE values in other years. It is also well noted that CropSow (Greenup) achieves much lower MBE in 2019 when extreme precipitation conditions occurred, suggesting that the Greenup metric holds the great potential in contributing to more stable and robust estimation of field-level planting dates. Considering that the better performance of CropSow (Greenup) manifests the greater stability and potential of this curvature-based remote sensing SOS metric, Greenup is selected as the phenological SOS indicator in the CropSow framework for the following analyses in this study.

The field-level planting date estimation results from the state-level CropSow framework are further aggregated and validated in the nine ASDs across Illinois, in an effort to obtain a more comprehensive understanding of the model performance. As mentioned before, CropSow (Greenup) is selected due to its better stability and accuracy. For each ASD, 200 randomly distributed corn fields are sampled, and the

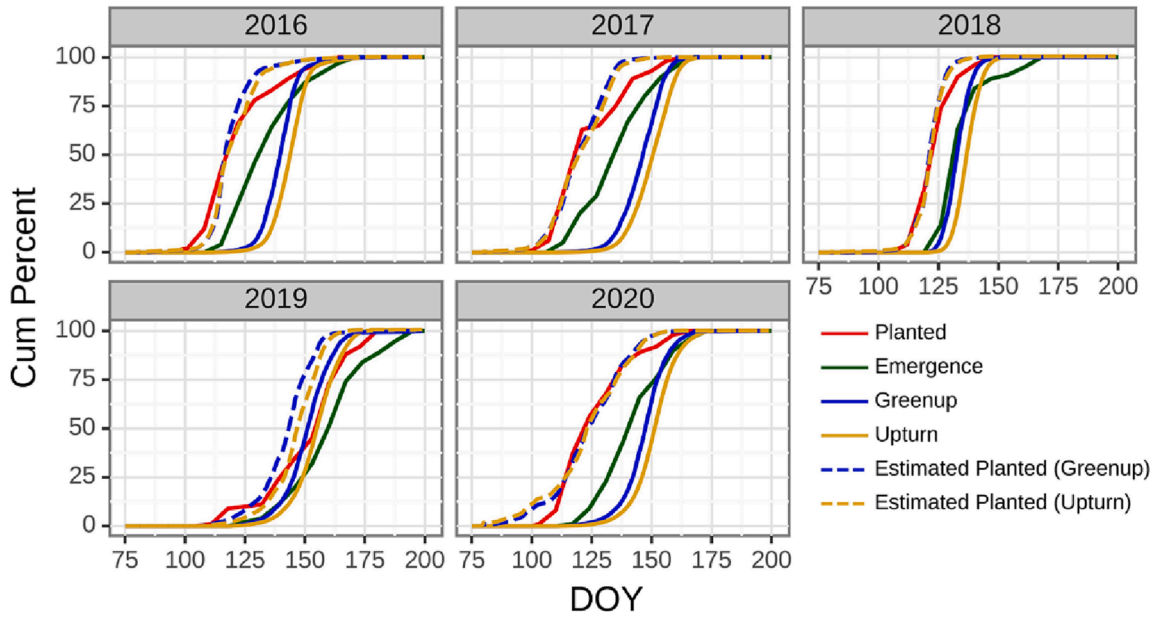

Fig. 8. Annual temporal cumulative distribution of emerged fields and planted fields from CPRs, Greenup and Upturn metrics extracted from MODIS imagery, and planting dates estimated by calibrated CropSow (Greenup or Upturn) in Illinois from 2016 to 2020.

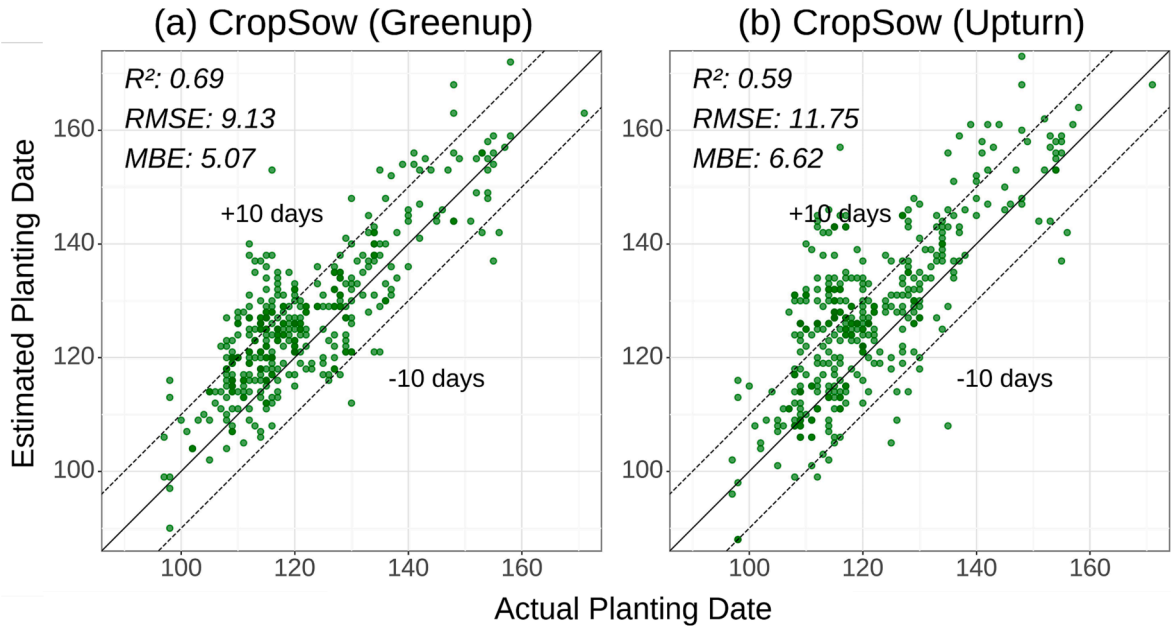

Fig. 9. Overall field-level planting date estimation results of CropSow using Greenup metric (a) and Upturn metric (b).

temporal cumulative distribution of those sampled fields is validated against the ASD-level CPRs. Given that the ASD-level CPRs are only available in 2016 and 2017 during the study period, only the estimation results in these two years are aggregated and analyzed. In general, the temporal cumulative distributions of estimated planting dates align with those of ASD-level CPRs in these two years, with comparable planting progress across ASDs (Fig. 11). The RMSEs between actual planting curves and estimated planting curves are <7 days in most ASDs, and the errors tend to be smaller around central Illinois. Specifically, RMSEs are all smaller than 7 days in 2016, except for the ESE (9.7 days) and SE (14.3 days) ASDs. The relatively large errors in these two ASDs are likely due to more disparate planting patterns (e.g., planting cumulative distributions) compared to the state-level planting pattern. In 2017, the RMSEs are relatively more homogeneous across the nine ASDs, with RMSE values mostly ranging from 6 to 9 days. The different temporal cumulative distributions of estimated planting dates also reflect the discrepancy of planting decisions made across different ASDs of Illinois with various environmental conditions. The overall agreement between estimated planting date distribution and regional statistics from CPRs confirms the feasibility of downscaling statistics data from state-level CPRs to higher spatial resolution through integrating remote sensing SOS metrics and crop growth models.

We further quantify the sensitivity of CropSow's performance to several input management variables (i.e., fertilizer, initial water, planting density, and planting depth) and our selected phenological parameter (i.e., *tt_emerg_to_sos*) for calibration. Specifically, we calculate the sensitivity index of each variable (or parameter) to evaluate its influence on CropSow's planting date estimation performance (Fig. 12).

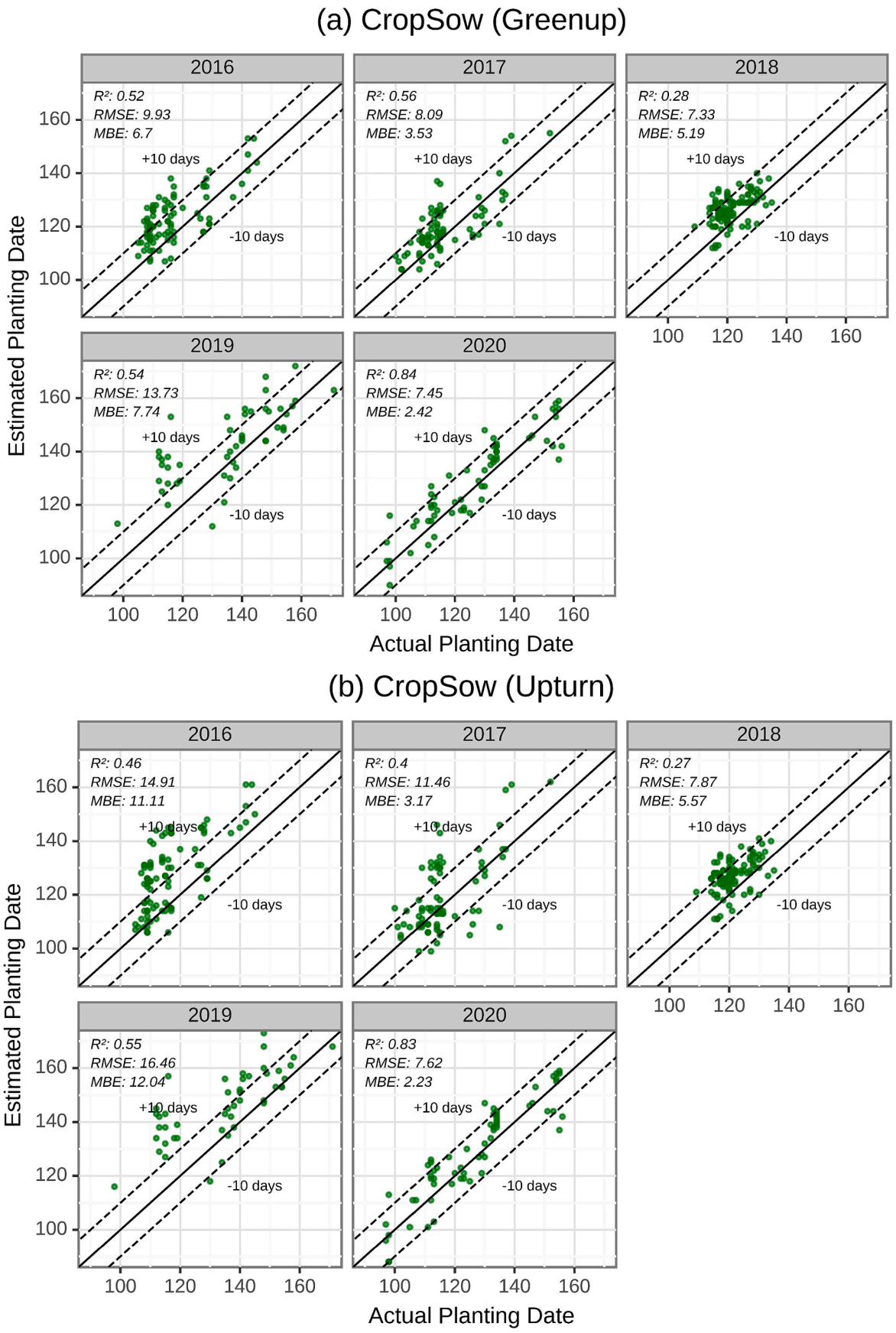

Fig. 10. Annual field-level planting date estimation results of CropSow (Greenup) (a) and CropSow (Upturn) (b).

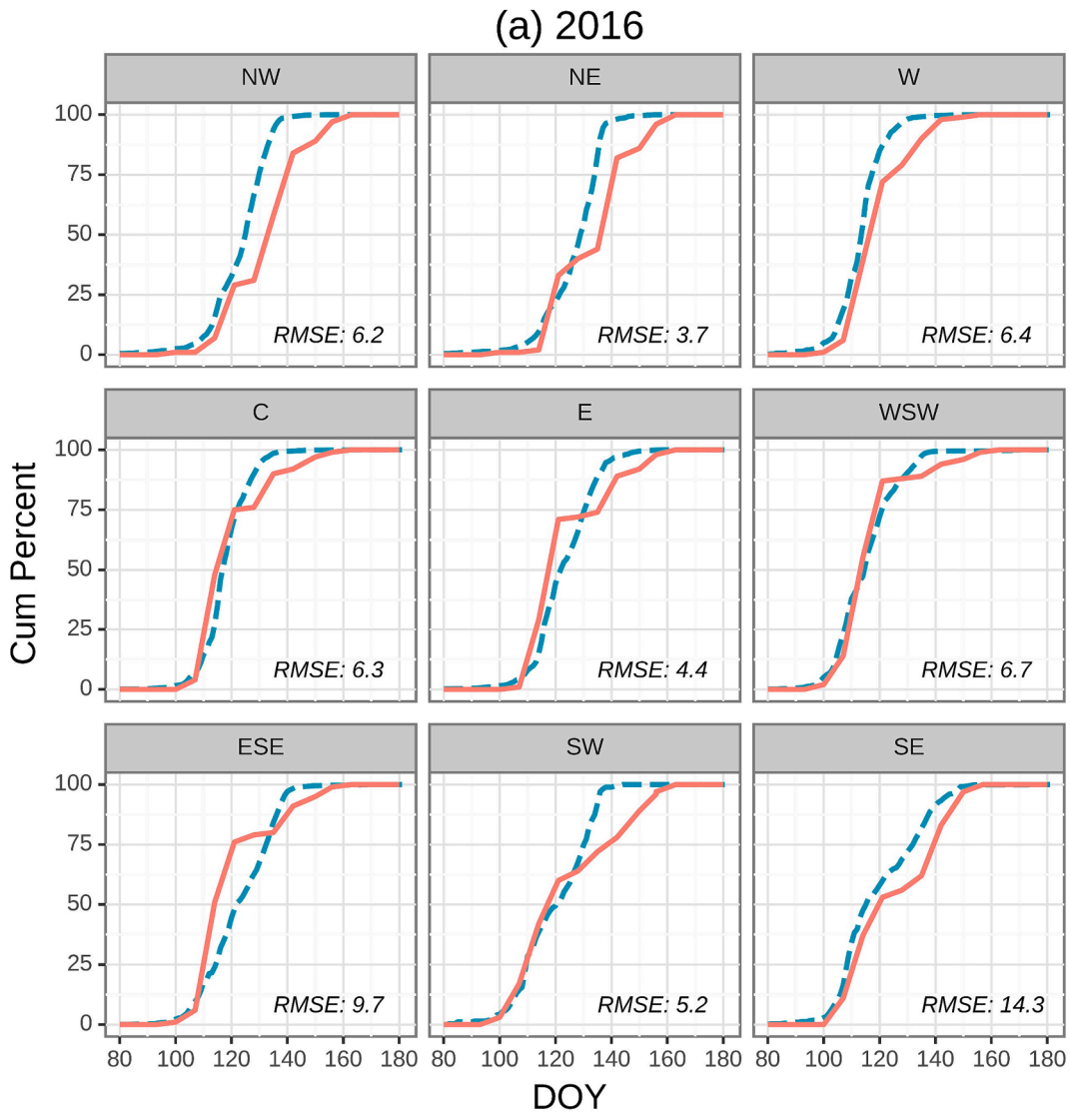

Fig. 11. ASD-level temporal cumulative distributions of planting dates estimated by CropSow (Greenup) (dashed blue lines) and those of actual planting dates from CPRs (solid red lines) in 2016 (a) and 2017 (b) for Illinois. (For interpretation of the references to colour in this figure legend, the reader is referred to the web version of this article.)

The main and total effect sensitivity indices show that the model performance is mostly affected by the calibration of *tt_emerg_to_sos* and is not that sensitive to input management variables. It confirms the validity of calibrating *tt_emerg_to_sos* in CropSow for planting date estimation.

4.2.2. Impacts of HLS image availability

While CropSow is able to retrieve field-level planting dates with generally satisfactory accuracy, the results of RMSEs and MBEs in Fig. 10 also suggest that the CropSow framework tends to estimate planting dates later than the actual ones for some corn fields. We examine the corresponding HLS NDVI time series of those overestimated fields, and hypothesize that the estimation error pattern may originate from the relatively scarce high-quality HLS images. To investigate the effect of HLS dataset's quality on planting date estimation performance, we define the planting date window as 30 days before and after the actual planting date of a given field. Then we count the number of high-quality HLS images during the planting date window for each field. Due to the late launch of the Sentinel 2B satellite in 2017, the high-quality HLS images in 2016 and the corresponding planting window are relatively scarcer than those in the next few years (Table 2).

We further analyze the impact of the number of high-quality HLS images within planting date windows on CropSow (Greenup) planting date estimation performance. Fig. 13 shows the boxplot of the absolute errors generated by CropSow (Greenup) with regard to the number of high-quality HLS images within the planting date window during the five years; the yellow lines represent the median of absolute error between actual and estimated planting dates; error bars represent the 95% confidence interval of absolute error between actual and estimated planting dates. In general, larger numbers of high-quality images around the actual planting date lead to lower absolute errors and more stable model performance (narrower range of fluctuations in absolute error). Thus, the degraded estimation accuracy can be explained by the lack of sufficient observations around the planting season, which likely causes inaccurate fitting process of the phenological time series and affects model performance. Though 2017 may lack high-quality HLS images in the planting date window, the overall larger number of HLS images for the whole year could help provide sufficient observations for the time series fitting process, ensuring relatively satisfactory model performance. In summary, sufficient high-quality satellite images in the growing season are critical for obtaining accurate planting date

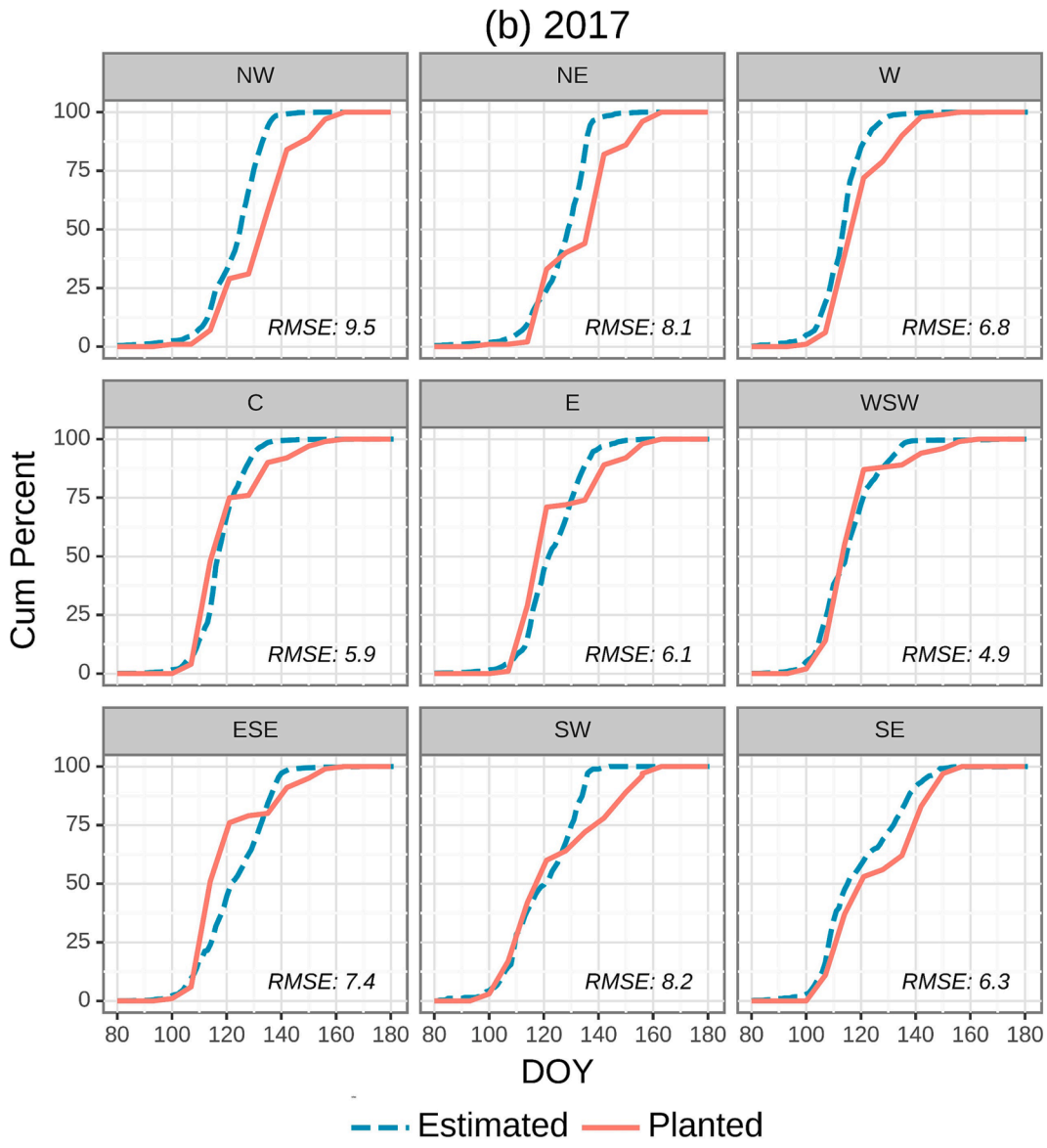

Fig. 11. (*continued*).

estimations at the field level.

4.2.3. Impacts of calibration dataset's spatial level

To evaluate the impacts of the calibration dataset's spatial levels on the performance of CropSow's estimation, we compare the planting date estimation performance of CropSow (Greenup) calibrated using ASD-level CPRs (ASD-level models) with that of CropSow calibrated using state-level CPRs (state-level models). The comparison is conducted for two of our study years, 2016 and 2017, during which a total of 18 ASD-level models are generated. Table 3 shows the field-level planting date estimation results of the ASD-level and state-level models. Pairwise *t*-test is performed to analyze the difference between the estimations generated by the two different spatial-level CropSow frameworks. The result ($p < 0.05$) suggests that ASD-level models exhibit significantly better performance compared to state-level models. Compared to state-level models, the overall MBE of ASD-level models decreases from 6.7 to 4.5 days in 2016 and from 3.5 to 1.6 days in 2017. The overall RMSE decreases from 9.9 to 8.6 days in 2016, and from 8.1 to 7.6 days in 2017. The advantage of the ASD-level models is more substantial for ASDs with more than ten validation fields. In 2016, the MBE decreases from 2.7 to −0.1 days in the NW ASD, from 8.3 to 5.8 days in the NE ASD, from 3.8 to 1.9 days in the W ASD, and from 8.9 to 5.5 days in the E ASD. In 2017, the MBE decreases from 3.9 to 0.6 days in the NW ASD, from 3.0 to 0.6 days in the C ASD, and from 1.8 to −0.7 days in the E ASD. The calibration of CropSow with more detailed ASD-level planting date statistics further accommodates the change of thermal time requirement from emergence to SOS metrics at a finer spatial level, leading to the improvement in estimation accuracy. Overall, a calibration dataset with a finer spatial level could facilitate a more accurate downscaling of regional planting date information and generate more satisfactory field-level planting date estimations.

4.3. Comparison of CropSow and benchmark models

Three state-of-the-art benchmark models are selected and compared with CropSow in terms of model performances on field-level planting date estimation. To be consistent with CropSow, all the benchmark models are calibrated with state-level CPRs and validated with Beck's field data. As shown in Fig. 14, CropSow shows the best performance in estimating field-level planting dates compared to the other three benchmark models in terms of R^2, RMSE, and MBE (0.69, 9.13, and 5.07, respectively). With the performance second only to CropSow, the remote

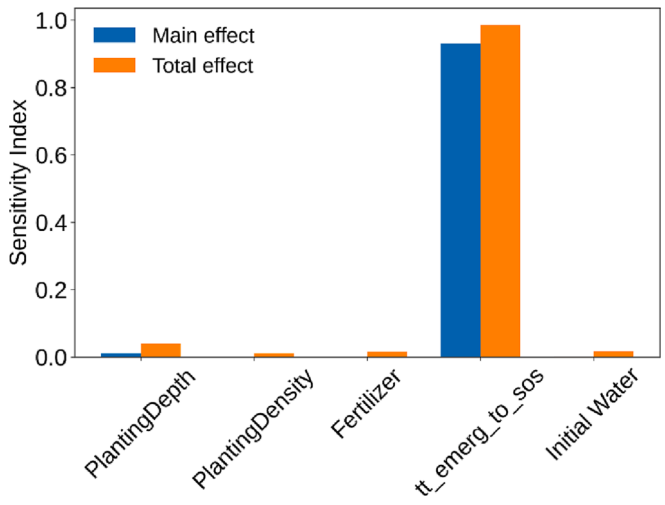

Fig. 12. The total and main effect sensitivity indices of four crop management input variables (i.e., fertilizer, initial water, planting density, and planting depth) and the key phenological parameter (*tt_emerg_to_sos*) calibrated in CropSow.

Table 2
Annual mean number of high-quality HLS images of Beck's fields for both whole year and planting window.

Temporal Range	2016	2017	2018	2019	2020
Whole Year	18	25	37	34	37
Planting Window	3	3	5	5	6

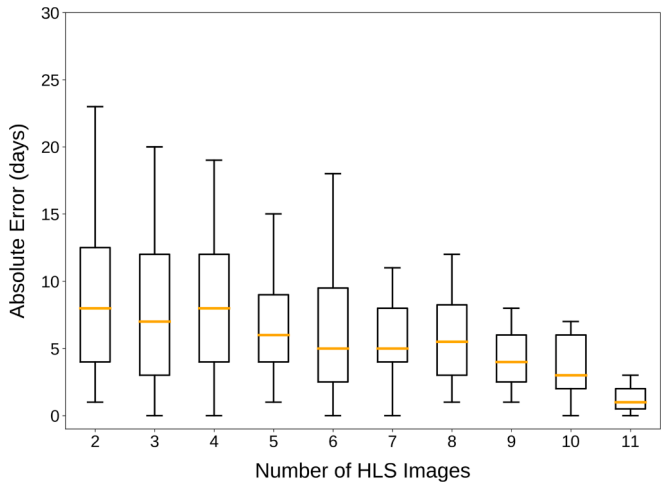

Fig. 13. The number of high-quality HLS images within the planting date window vs the absolute error of planting dates estimated by CropSow (Greenup). The yellow lines represent the median of absolute error between actual and estimated planting dates. Error bars are the 95% confidence interval of absolute error between actual and estimated planting dates. (For interpretation of the references to colour in this figure legend, the reader is referred to the web version of this article.)

sensing AGDD method achieves a relatively satisfactory result with R^2 of 0.66, RMSE of 11.23 days, and MBE of 7.11 days. Shape model ranks the third with R^2 of 0.44, RMSE of 13.73 days, and MBE of 9.04 days. While these three methods' estimates at the field level are all relatively aligned with the in-situ planting data, CropSow is able to produce the results with less overestimation. This advantage can be partially attributed to the introduction of the APSIM in CropSow. The weather-dependent method gives a relatively poorer field-level planting date estimation performance with respect to its R^2 and RMSE (0.02 and 18.24, respectively), yet it produces a relatively small MBE (4.08 days). Different from the other three models (Fig. 14(a)–(c)), the weather-dependent model generates data points that are evenly distributed on both sides of the diagonal (Fig. 14(d)). The small MBE also indicates that the weather-dependent model can capture the general planting timing across the state. However, Fig. 14(d) alongside the R^2 and RMSE values reveals that the weather-related variables cannot explain the variation of planting dates at the field level.

From the perspective of annual estimation results, CropSow performs consistently better than the benchmark models during the study period, with its RMSE values ranging from 7.3 to 13.3 days, MBE values ranging from 2.4 to 7.7 days, and R^2 values ranging from 0.28 to 0.84 (Fig. 15). In 2019, CropSow shows stronger adaptability to extreme weather conditions than benchmark models, likely due to the consideration of soil-crop-atmosphere interaction in APSIM. The remote sensing AGDD method yields the best estimation accuracy among the three benchmark models in all the five years, with RMSE values ranging from 7.9 to 19.2 days, MBE values ranging from 3.9 to 15.7 days, and R^2 values around 0.5. The shape model generates relatively higher RMSE and MBE values and lower R^2 values than CropSow and the remote sensing AGDD method. The weather-dependent method generates the highest RMSE in most years and the lowest R^2 in all the years. It exhibits extreme fluctuations and uncertainties in planting date estimations among the study years. The lowest MBEs in 2016, 2018 and 2019 reindicate that the weather-dependent model can capture the general planting timing across the state. Overall, these results demonstrate the ability of CropSow to provide reliable field-level planting date estimations under various weather conditions across the five years.

To further evaluate the generalizability of the CropSow framework, we estimate the field-level planting dates for one year (the target year) using state-level CropSow (Greenup) framework calibrated with other years data. Among the benchmark models, the remote sensing AGDD method achieves the best performance and is thus compared with the CropSow framework. Fig. 16 displays the planting date estimation results under three scenarios. Firstly, the CropSow framework is calibrated and evaluated using the same year's data (scenario 1). Secondly, the CropSow framework is calibrated and evaluated using different years' data (scenario 2). Thirdly, the remote sensing AGDD method is calibrated and evaluated using different years' data (scenario 3). For these three scenarios, scenario 1 achieves a better performance in field-level planting date estimation than scenario 2. Among these five years, the MBEs values stabilize at around 5 days under scenario 1 and the RMSE values are mostly lower than 10 days. Though degraded performance is observed under scenario 2, CropSow calibrated with other years' data can still control the MBE and RMSE values within two weeks in all the years except 2017. When both calibrated with the different years' data, CropSow (scenario 2) shows consistently better stability and accuracy than the remote sensing AGDD method (scenario 3). The R^2 values under scenario 2 are consistently higher than those under scenario 3 except in 2018. Scenario 2 also produces lower MBEs and RMSEs than scenario 3 for almost all the years. The consistent advantage indicates the higher potential generalizability of the CropSow framework. Through the incorporation of physiological mechanisms, CropSow achieves higher scalability when it is applied to estimate the planting dates in other years that are different from the framework's calibration year.

4.4. Field-level planting date mapping

Using the CropSow framework, we produce the field-level corn planting date maps for the counties of Champaign and Dekalb alongside their corresponding temporal cumulative distributions of planting dates from 2016 to 2020 (Fig. 17). These maps reveal the spatiotemporal variability of planting dates among cropland field parcels, with a more significant change of planting dates observed across years than locations. From the temporal cumulative distributions, the trend of planting

Table 3
Field-level planting date estimation results using CropSow (Greenup) calibrated by state-level and ASD-level CPRs, respectively (The ASDs with more than 10 Beck's fields are in bold).

	2016				2017			
	State-CPR		ASD-CPR		State-CPR		ASD-CPR	
	RMSE	MBE	RMSE	MBE	RMSE	MBE	RMSE	MBE
NW	**9.0**	**2.7**	**9.8**	**−0.1**	**9.1**	**3.9**	**8.4**	**0.6**
NE	**13.1**	**8.3**	**11.7**	**5.8**	11.4	7.6	9.8	4.8
W	**5.8**	**3.8**	**4.8**	**1.9**	5.4	−2.0	4.7	2.0
C	11.9	10.9	8.8	7.5	**6.7**	**3.0**	**5.9**	**0.6**
E	**10.5**	**8.9**	**7.7**	**5.5**	**8.8**	**1.8**	**8.8**	**−0.7**
WSW	9.5	5.2	8.4	3.2	7.4	4.4	7.4	4.0
ESE	8.3	5.9	10.8	9	12.8	12.5	8.2	7.5
SW	NA	NA	NA	NA	6.4	5.7	7.7	7.0
SE	1.0	1.0	7.0	7.0	5.4	2.0	8.2	6.0
Overall	**9.9**	**6.7**	**8.6**	**4.5**	**8.1**	**3.5**	**7.6**	**1.6**

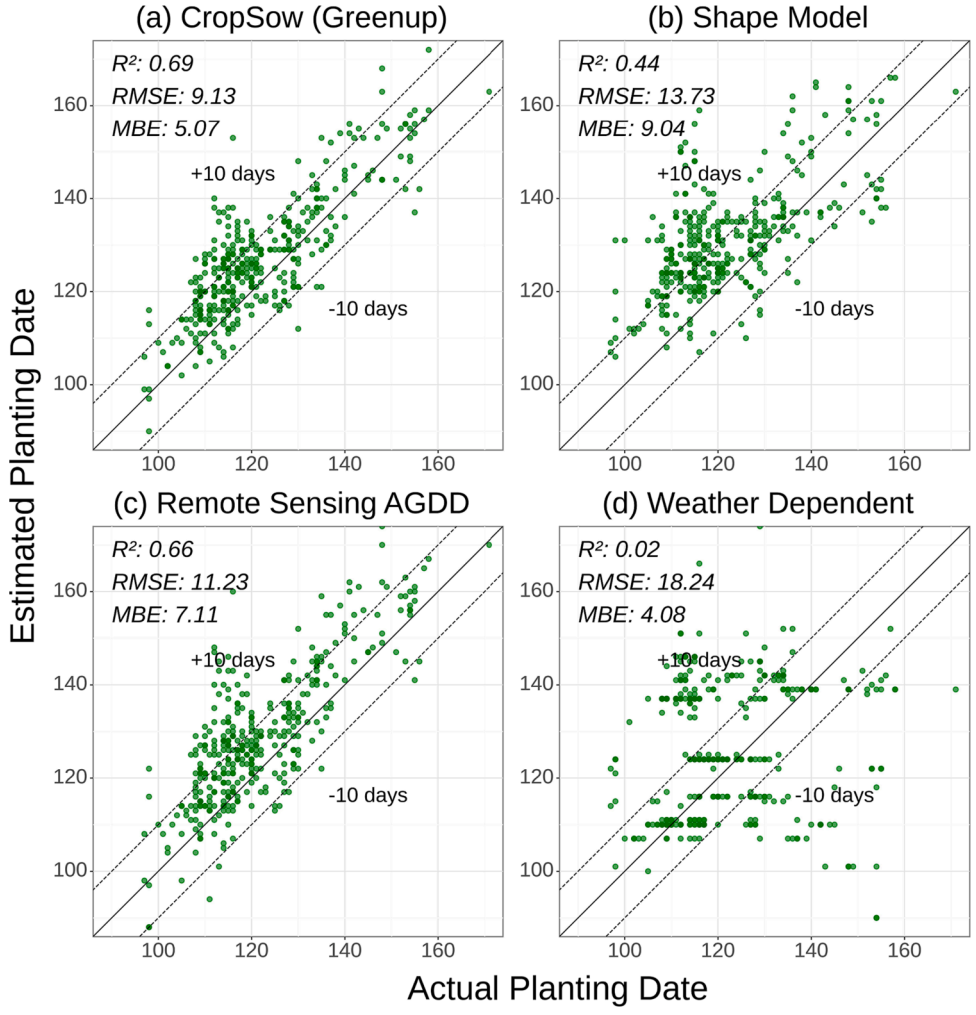

Fig. 14. Overall field-level planting date estimation results of CropSow (Greenup) (a), shape model (b), remote sensing AGDD method (c), and weather-dependent method (d) calibrated using state-level CPRs from 2016 to 2020.

dates varies during these five years. In 2018, planting dates are densely distributed in a relatively short three-week window from DOY 120 to DOY 140 for these two counties, showing the effect of extreme temperature swings on planting management. As a result of the excessive precipitation in spring, planting in 2019 mainly occurs after DOY 140, which is much later than that in other years. In 2020, these two counties experience more considerable variations in planting dates compared to other years, reflecting varying farmers' decisions on planting management under the rapidly changing situation with the spread of COVID-19 and its attendant health threats in that year (Schnitkey et al., 2020). The annual maps show that the planting dates are generally later in Dekalb than those in Champaign in these years. Such later planting decisions in the Dekalb county are resulted from its higher latitude and lower temperature. Overall, the CropSow framework demonstrates its capability in capturing field-level spatial and temporal variability of the estimated planting dates, and the model derived variability patterns are

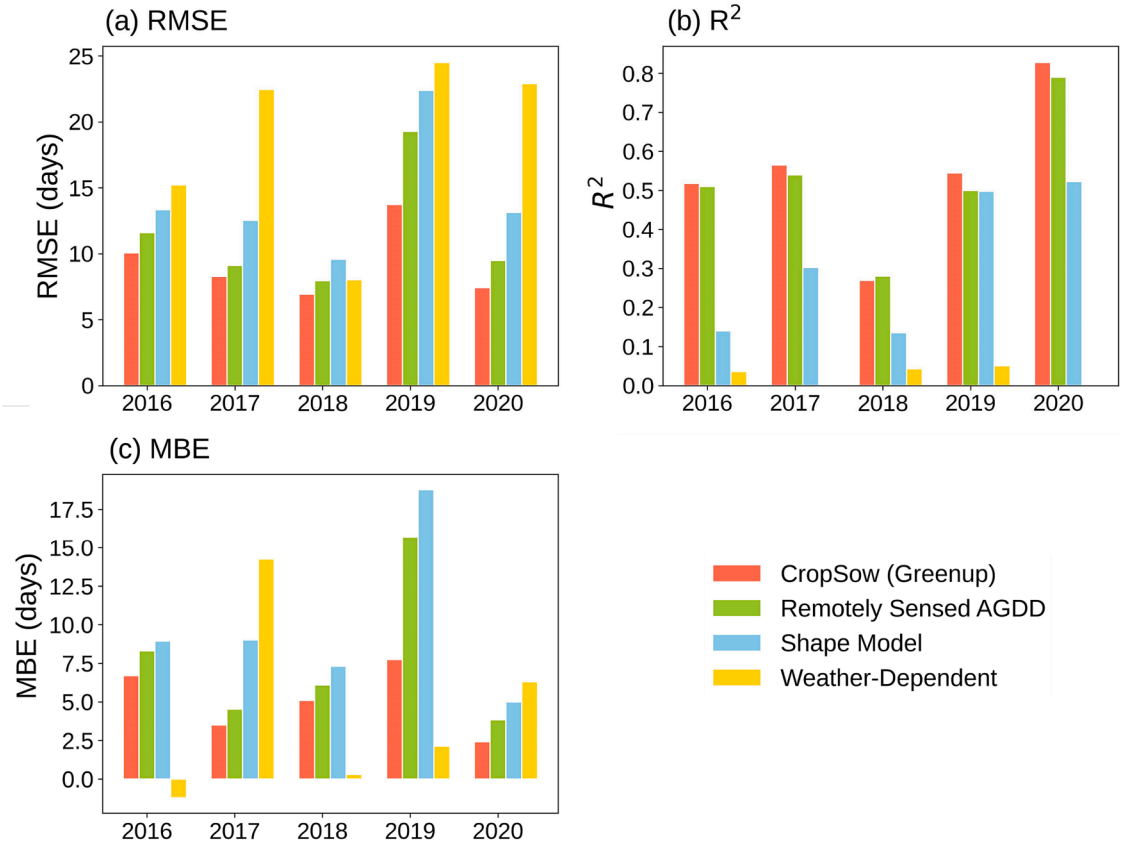

Fig. 15. RMSE (a), R^2 (b), and MBE (c) of annual field-level planting date estimation results among CropSow (Greenup) and three benchmark models.

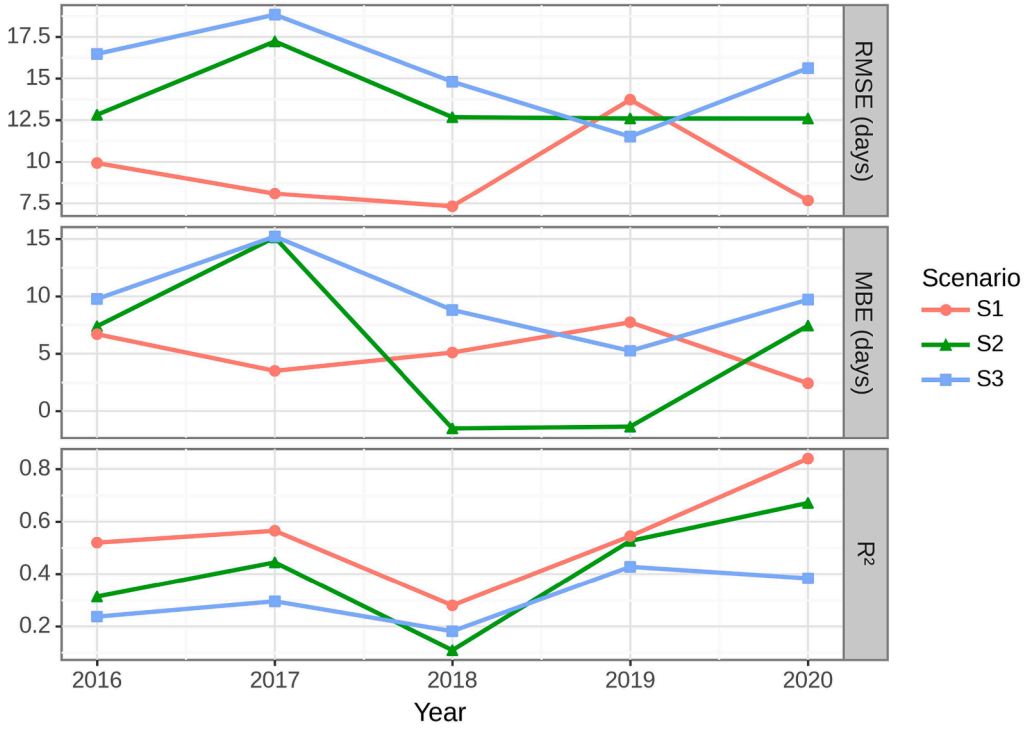

Fig. 16. Field-level planting date estimation accuracy measures (RMSE, MBE, and R^2) across five years under three scenarios. Scenario 1 (S1): CropSow (Greenup) framework is calibrated and evaluated using the same year's data; scenario 2 (S2): CropSow (Greenup) framework is calibrated and evaluated using different years' data; scenario 3 (S3): Remote Sensing AGDD method is calibrated and evaluated using different years' data.

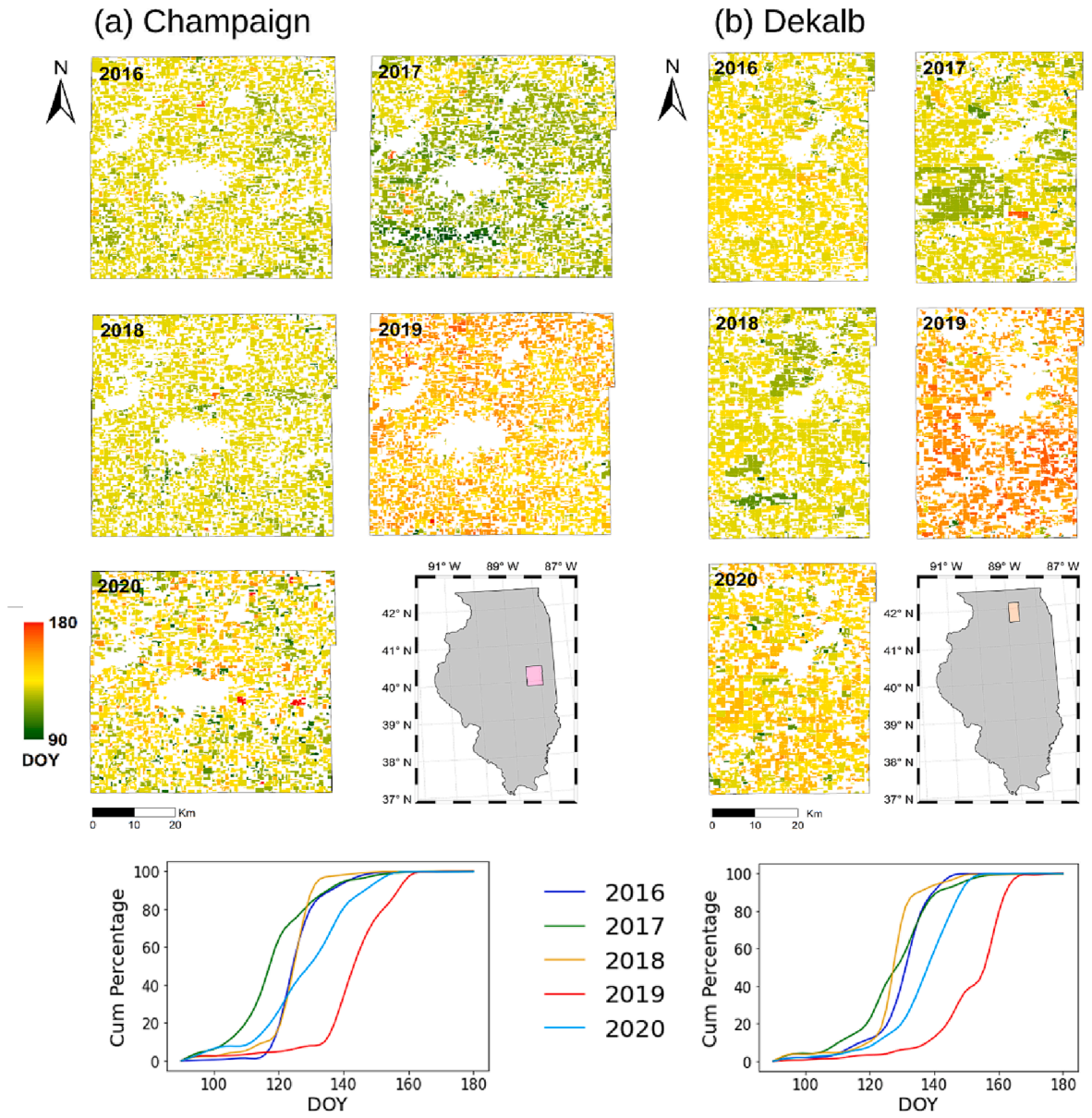

Fig. 17. Corn field-level planting date maps estimated by CropSow (Greenup) for the counties of (a) Champaign and (b) Dekalb from 2016 to 2020 with their corresponding county-level temporal distributions of planting dates.

generally consistent with our understanding of the different planting practices during the five years of the study period. The mapping results further confirm CropSow's ability to accurately estimate field-level planting dates, which can largely be attributed to the utilization of spatially explicit NDVI time series for individual fields and the consideration of the interactions among crop types, crop management, and environment.

5. Discussion

In this study, we develop a novel CropSow modeling framework to estimate the crop planting dates at the field level by integrating the remote sensing phenological detecting method and the crop growth model. The remote sensing phenological detecting method encompasses the time series phenological pre-processing, time series phenological fitting, and time series phenological characterization. With a suite of methods devised to remove the spurious and abnormal observations of NDVI time series, as well as diminishing the influence of off-season vegetation (e.g., weeds and cover crops), the phenological profile of the target crop can be extracted and modeled to retrieve the SOS phenological metrics. As both curvature-based Greenup and GU-based Upturn SOS metrics have been demonstrated to approximate the corn initial vegetative stage (e.g., corn V3 stage with about 2–4 leaves), these two SOS metrics have been retrieved in this study via the remote sensing phenological detecting method for the subsequent integration into the crop growth model for corn planting date estimation. Compared to the GU-based Upturn metric, CropSow with the curvature-based Greenup metric achieves higher accuracy in estimating the corn planting dates at the field level. The Greenup metric is retrieved via the change rate of the curvature, whereas the Upturn metric is extracted via the intersection between the recovery line and base line of the fitted NDVI time series curve (Fig. 4). The use of several curves may bring more uncertainties in the GU-based phenological metric retrieval, which further affects the performance of CropSow. The good performance of the curvature-based Greenup metric in detecting crop phenology has also been suggested by previous studies (Diao and Li, 2022).

The crop growth model in CropSow further enables the comprehensive modeling of crop phenological development in consideration of

soil-crop-atmosphere continuum. It takes into account a variety of weather, soil, and management factors to model the phenological progress from corn planting to germination, germination to emergence, as well as emergence to SOS stages. The integration of the remote sensing phenological detecting method and the crop growth model thus enables CropSow to estimate crop planting dates under varying environmental and management conditions. By accommodating the complex soil-crop-atmosphere interactive process underlying crop physiological growth, CropSow shows unique strength particularly in field-level planting date estimation. It can capture the spatiotemporal variation in field-level crop phenological development by integrating the field-specific remotely sensed crop growth signals and the associated field environmental characteristics. The calibration of crop growth model in CropSow facilitates the downscaling of the regional aggregated crop planting information to the field level with farm-tailored planting information. The global sensitivity analysis of crop growth model further indicates that the model performance is mostly affected by the calibration of the phenological parameter *tt_emerg_to_sos* and is substantially less sensitive to crop management inputs. This is consistent with the mechanism underlying corn plant growth that these crop management practices mainly influence simulations of corn phenology after the end of the juvenile stage as well as subsequent crop yield, rather than initial corn phenology (Peng et al., 2018). The sensitivity analysis demonstrates the importance of calibrating *tt_emerg_to_sos* in CropSow, as well as the potential in estimating field-level planting dates when accurate crop management inputs are not readily available. Given the state-level CPRs publicly accessible in the US, CropSow holds strong promise to systematically conduct field-level crop planting date estimations at large scales with the CPR-enabled calibration and downscaling. The ASD-level CPRs for defined regions and years might further improve the corresponding field planting date estimations, given the potential influence of calibration dataset's spatial level. Owing to the consideration of the physiological mechanism, CropSow also shows stronger adaptability than other approaches to abnormal weather conditions (e.g., excessive rainfall in 2019) with more stable and accurate estimations of field-level planting dates.

Among the three benchmark methods, the remote sensing AGDD method achieves higher accuracy in field-level planting date estimation with the consideration of the thermal time accumulation in the crop growth process. As a measure of heat accumulation, AGDD is used to quantify the plant development rate and is a major factor determining crop phenological growth. The time lag between planting dates and remote sensing SOS metrics can be estimated in terms of AGDD to infer the planting dates. Compared to the calendar-based time lag, the AGDD-based one exhibits significantly lower normalized variance of all the corn fields of Beck's dataset ($p < 0.001$), according to the Brown-Forsythe test (Fig. S3). This finding indicates the advantage of AGDD over calendar length in representing the time lag between SOS and planting time. However, the crop phenological progress from planting to SOS encompasses several stages (e.g., germination and emergence), with the duration of each stage affected by a combination of environmental and management factors. Despite the important role of AGDD, other factors (e.g., soil conditions and water stress) may also affect the crop phenological development. CropSow is able to simulate the crop phenological development from planting to SOS with comprehensive consideration of crop thermal time requirement, crop management practices, as well as water and nitrogen stress. The superior performance of CropSow over the remote sensing AGDD method further demonstrates the importance of accommodating the complex soil-crop-atmosphere interactive process in conducting the planting date estimations at the field level.

As a rule-based method, the weather-dependent method shows potential in capturing the general crop planting timing at the regional scale, but is challenging in estimating the planting dates of individual farm fields. This challenge may partly be explained by the subjective decisions of farmers on crop management in practice. Even under suitable environmental conditions, farmers may postpone the planting practices due to the machine unavailability. The weather-dependent method thus exhibits large fluctuations and uncertainties in field-level planting date estimation. Yet compared to other methods that leverage remotely sensed crop growth signals, the weather-dependent method may be more suitable for estimating crop planting dates in a near-real time manner. With a priori crop reference phenological time series and reference planting date, the shape model can estimate the planting date of the target time series via the geometrical matching. Despite the flexibility in potentially estimating any phenological stages with corresponding reference, the shape model may have limited capability in estimating the planting dates of individual farm fields. On one hand, the formulation (or calibration) of reference phenological profile and reference planting date remains a significant challenge in phenology matching models (Sakamoto, 2018; Liu et al., 2022). On the other hand, the pre-defined phenological reference templates may not adequately adapt to the target farm fields for phenological retrievals, particularly for the planting stage that is subject to management decisions. The shape model thus may not perform as well as CropSow and the remote sensing AGDD method in field-level planting date estimations, yet outperforms the weather-dependent method in this study.

The CropSow framework also demonstrates good performance in estimating the field-level planting dates in the years that are different from the framework's calibration year. Under the scenario of the lack of target year's calibration data, CropSow exhibits a stronger temporal generalization capability than the remote sensing AGDD method. It indicates that simulating crop phenological progress with the consideration of soil-crop-atmosphere interactive process can make the planting date estimation more robust in comparison with only the consideration of AGDD. We further evaluate the spatial generalization ability of CropSow by calibrating the framework using the CPR of one representative ASD (East) and evaluating the planting date estimation performance in all ASDs of Illinois. Comparable estimation performance is achieved across all the nine ASDs (Table S2), indicating good spatial generalization ability of CropSow across Illinois. In future studies, the generalization ability of CropSow for farm field planting date estimations can further be evaluated over extended regions (e.g., US corn belt).

Despite the strength of CropSow in field-level planting date estimation, the simultaneous use of remote sensing and crop growth model may potentially bring uncertainty to the estimation results. Given the impact of the availability of HLS images (particularly around the planting window) on planting estimation accuracies, fusion of HLS and MODIS images to generate temporally dense observations (e.g., daily temporal resolution) at the 30 m spatial resolution can be explored in future studies. The limited HLS observations may potentially affect the process of phenological fitting and cause a bias in extracting corresponding remote sensing phenological metrics. By fusing the high-spatial-low-temporal-resolution images (e.g., HLS) and high-temporal-low-spatial-resolution images (e.g., MODIS) to generate the images of both high spatial and temporal resolutions, the spatiotemporal image fusion methods can help reduce uncertainty from remote sensing to facilitate the field-level crop phenological monitoring (Yang et al., 2021; Sadeh et al., 2021; Zhu et al., 2022). Additionally, the calibration of CropSow as well as three benchmark methods using state-level planting date information may introduce bias to field-level planting date estimation. The overall delayed estimation of planting dates of reference corn fields may partly be due to the uncertainty in the downscaling process (e.g., environmental and planting practice uncertainty) as well as the potential bias (e.g., survey bias) in CPRs. Calibrating the CropSow framework with in-situ field-level planting date and phenological stage information would be desired in future to reduce the calibration and downscaling bias, yet the collection of a large number of in-situ field-level phenological data over large scales could be challenging. With the comprehensive mechanisms embedded in crop growth models for simulating crop growth and phenological development, the complexity of crop models might potentially bring uncertainty to the estimation

results, particularly the need of crop management data. The sensitivity analysis of APSIM in this study facilitates the evaluation of the influence of crop input management variables on model performance. Despite relatively low sensitivity index values, the uncertainty caused by varying crop management inputs in planting date estimations could be further evaluated.

With the essential environmental conditions affecting crop planting and subsequent phenological development accommodated in CropSow, the devised framework holds strong potential in mapping field-level crop planting dates at large scales. Future investigations of other crops over extended geographical regions will be desired for more comprehensive planting date mapping across the US. The spatial distribution of the field-level planting date maps can be utilized to explore the potential effect of climate change on crop management practices of individual farm fields. Along with field-level crop yield maps, the field-level planting maps can provide auxiliary data sources to analyze the potential reasons of crop yield gaps among the cropland fields, especially for those fields with different planting patterns. The assessment of the gaps between achieved and achievable yields can enable more profitable and sustainable farm management adaptations, as well as more effective policy decisions for addressing food insecurity. Furthermore, the CropSow framework holds potential for in-season planting date estimation. As the first logistic curve of the Beck's method can be fitted using the remote sensing data up to the period of corn tasseling or silking, the SOS metrics could be extracted accordingly to facilitate more prompt decision-making by farmers and policymakers.

6. Conclusions

In this study, we develop an innovative CropSow framework that integrates the remote sensing phenological detecting method and the crop growth model to robustly estimate planting dates of corn fields under varying soil and weather conditions. The CropSow framework is evaluated alongside three benchmark methods (the remote sensing AGDD method, the weather-dependent method, and the shape model). With its integrative remote sensing and crop physiological design, CropSow demonstrates its enhanced capability in accurately estimating planting dates of corn fields without field-level ground truth data for calibration. In Illinois, CropSow with the Greenup metric can estimate planting dates of corn fields with R^2 higher than 0.68, RMSE lower than 10 days, and MBE around 5 days from 2016 to 2020. It shows stronger adaptability than the benchmark methods to abnormal weather conditions with more robust performance, as well as stronger generalizability than the benchmark method of best performance (i.e., the remote sensing AGDD method). The estimated field-level crop planting dates can provide valuable information for more accurate simulations of crop growth models and the analysis of the underlying reason for yield gaps at the field level. The spatiotemporal patterns of planting dates can help design proactive adaptation strategies to overcome the negative effect of climate change.

Declaration of Competing Interest

The authors declare that they have no known competing financial interests or personal relationships that could have appeared to influence the work reported in this paper.

Acknowledgements

Funding support for this research is provided by the National Science Foundation (grant number 2048068), the National Aeronautics and Space Administration (grant number 80NSSC21K0946), and the United States Department of Agriculture (grant number 2021-67021-33446). The authors would also like to acknowledge the funding support from the Geospatial Institute Seed Grant Program to stimulate Collaborative Research (GISCoR) of Taylor Geospatial Institute managed by Saint Louis University.

Appendix A. Supplementary material

Supplementary data to this article can be found online at https://doi.org/10.1016/j.isprsjprs.2023.06.012.

References

Asseng, S., Zhu, Y., Basso, B., Wilson, T., Cammarano, D., 2014. In: Encyclopedia of Agriculture and Food Systems. Elsevier, pp. 102–112.

Baum, M.E., Licht, M.A., Huber, I., Archontoulis, S.V., 2020. Impacts of climate change on the optimum planting date of different maize cultivars in the central US Corn Belt. Eur. J. Agron. 119 (September), 126101 https://doi.org/10.1016/j.eja.2020.126101.

Beck, P.S.A., Atzberger, C., Høgda, K.A., Johansen, B., Skidmore, A.K., 2006. Improved monitoring of vegetation dynamics at very high latitudes: a new method using MODIS NDVI. Remote Sens. Environ. 100 (3), 321–334. https://doi.org/10.1016/j.rse.2005.10.021.

Beddington, J., 2010. Food security: contributions from science to a new and greener revolution. Philos. Trans. R. Soc., B 365 (1537), 61–71. https://doi.org/10.1098/rstb.2009.0201.

Birch, C.J., Vos, J., Kiniry, J., Bos, H.J., Elings, A., 1998. Phyllochron responds to acclimation to temperature and irradiance in Maize. Field Crop Res 59 (3), 187–200. https://doi.org/10.1016/S0378-4290(98)00120-8.

Boryan, C., Yang, Z., Mueller, R., Craig, M., 2011. Monitoring US agriculture: the US department of agriculture, national agricultural statistics service, cropland data layer program. Geocarto. Int. 26 (5), 341–358. https://doi.org/10.1080/10106049.2011.562309.

Brisson, N., Mary, B., Ripoche, D., Jeuffroy, M.H., Ruget, F., Nicoullaud, B., Gate, P., Devienne-Barret, F., Antonioletti, R., Durr, C., Richard, G., Beaudoin, N., Recous, S., Tayot, X., Plenet, D., Cellier, P., Machet, J.-M., Meynard, J.M., Delécolle, R., 1998. STICS: a generic model for the simulation of crops and their water and nitrogen balances. I. Theory and parameterization applied to wheat and corn. Agronomie 18 (5–6), 311–346. https://doi.org/10.1016/S1161-0301(02)00110-7.

Brisson, N., Gary, C., Justes, E., Roche, R., Mary, B., Ripoche, D., Zimmer, D., Sierra, J., Bertuzzi, P., Burger, P., Bussière, F., Cabidoche, Y.M., Cellier, P., Debaeke, P., Gaudillère, J.P., Hénault, C., Maraux, F., Seguin, B., Sinoquet, H., 2003. An overview of the crop model stics. Eur. J. Agron. 18 (3–4), 309–332. https://doi.org/10.1016/S1161-0301(02)00110-7.

Challinor, A.J., Watson, J., Lobell, D.B., Howden, S.M., Smith, D.R., Chhetri, N., 2014. A meta-analysis of crop yield under climate change and adaptation. Nat. Clim. Chang. 4 (4), 287–291. https://doi.org/10.1038/nclimate2153.

Chen, J., Jönsson, P., Tamura, M., Gu, Z., Matsushita, B., Eklundh, L., 2004. A simple method for reconstructing a high-quality NDVI time-series data set based on the Savitzky-Golay Filter. Remote Sens. Environ. 91 (3–4), 332–344. https://doi.org/10.1016/j.rse.2004.03.014.

Choi, Y.-S., Gim, H.-J., Ho, C.-H., Jeong, S.-J., Park, S.K., Hayes, M.J., 2017. Climatic influence on corn sowing date in the midwestern United States: climatic influence on corn sowing date. Int. J. Climatol. 37 (3), 1595–1602. https://doi.org/10.1002/joc.4799.

Covell, S., Ellis, R.H., Roberts, E.H., Summerfield, R.J., 1986. The influence of temperature on seed germination rate in grain legumes: I. A comparison of chickpea, lentil, soyabean and cowpea at constant temperatures. J Exp Bot 37 (5), 705–715. https://doi.org/10.1093/jxb/37.5.705.

Delbart, N., Le Toan, T., Kergoat, L., Fedotova, V., 2006. Remote sensing of spring phenology in boreal regions: a free of snow-effect method using NOAA-AVHRR and SPOT-VGT Data (1982–2004). Remote Sens. Environ. 101 (1), 52–62. https://doi.org/10.1016/j.rse.2005.11.012.

Diao, C., 2020. Remote sensing phenological monitoring framework to characterize corn and soybean physiological growing stages. Remote Sens. Environ. 248 (October), 111960 https://doi.org/10.1016/j.rse.2020.111960.

Diao, C., Li, G., 2022. Near-surface and high-resolution satellite time series for detecting crop phenology. Remote Sens. (Basel) 14 (9), 1957. https://doi.org/10.3390/rs14091957.

Diao, C., Yang, Z., Gao, F., Zhang, X., Yang, Z., 2021. Hybrid phenology matching model for robust crop phenological retrieval. ISPRS J. Photogramm. Remote Sens. 181 (November), 308–326. https://doi.org/10.1016/j.isprsjprs.2021.09.011.

Dobor, L., Barcza, Z., Hlásny, T., Árendás, T., Spitkó, T., Fodor, N., 2016. Crop planting date matters: estimation methods and effect on future yields. Agric. For. Meteorol. 223 (June), 103–115. https://doi.org/10.1016/j.agrformet.2016.03.023.

Dong, T., Shang, J., Qian, B., Liu, J., Chen, J.M., Jing, Q.i., McConkey, B., Huffman, T., Daneshfar, B., Champagne, C., Davidson, A., MacDonald, D., 2019. Field-scale crop seeding date estimation from MODIS data and growing degree days in Manitoba, Canada. Remote Sens. (Basel) 11 (15), 1760. doi.org/10.3390/rs11151760.

Dos Santos, C.L., Abendroth, L.J., Coulter, J.A., Nafziger, E.D., Suyker, A., Yu, J., Schnable, P.S., Archontoulis, S.V., 2022. Maize leaf appearance rates: a synthesis from the united states corn belt. Front. Plant Sci. 13 https://doi.org/10.3389/fpls.2022.872738.

Gao, F., Anderson, M.C., Zhang, X., Yang, Z., Alfieri, J.G., Kustas, W.P., Mueller, R., Johnson, D.M., Prueger, J.H., 2017. Toward mapping crop progress at field scales through fusion of landsat and MODIS imagery. Remote Sens. Environ. 188 (January), 9–25. https://doi.org/10.1016/j.rse.2016.11.004.

Gu, L., Post, W.M., Baldocchi, D.D., Black, T.A., Suyker, A.E., Verma, S.B., Vesala, T., Wofsy, S.C., 2009. In: Phenology of Ecosystem Processes. Springer, New York, New York, NY, pp. 35–58.

Gümüşçü, A., Tenekeci, M.E., Bilgili, A.V., 2020. Estimation of wheat planting date using machine learning algorithms based on available climate data. Sust. Comput. Inf. Syst. 28 (December), 100308 https://doi.org/10.1016/j.suscom.2019.01.010.

Heng, L.K., Hsiao, T., Evett, S., Howell, T., Steduto, P., 2009. Validating the FAO AquaCrop model for irrigated and water deficient field maize. Agron. J. 101 (3), 488–498. https://doi.org/10.2134/agronj2008.0029xs.

Holzworth, D.P., Huth, N.I., deVoil, P.G., Zurcher, E.J., Herrmann, N.I., McLean, G., Chenu, K., van Oosterom, E.J., Snow, V., Murphy, C., Moore, A.D., Brown, H., Whish, J.P.M., Verrall, S., Fainges, J., Bell, L.W., Peake, A.S., Poulton, P.L., Hochman, Z., Thorburn, P.J., Gaydon, D.S., Dalgliesh, N.P., Rodriguez, D., Cox, H., Chapman, S., Doherty, A., Teixeira, E., Sharp, J., Cichota, R., Vogeler, I., Li, F.Y., Wang, E., Hammer, G.L., Robertson, M.J., Dimes, J.P., Whitbread, A.M., Hunt, J., van Rees, H., McClelland, T., Carberry, P.S., Hargreaves, J.N.G., MacLeod, N., McDonald, C., Harsdorf, J., Wedgwood, S., Keating, B.A., 2014. APSIM – evolution towards a new generation of agricultural systems simulation. Environ. Model. Softw. 62, 327–350. https://doi.org/10.1016/j.envsoft.2014.07.009.

Huang, J., Gómez-Dans, J.L., Huang, H., Ma, H., Wu, Q., Lewis, P.E., Liang, S., Chen, Z., Xue, J.-H., Wu, Y., Zhao, F., Wang, J., Xie, X., 2019. Assimilation of remote sensing into crop growth models: current status and perspectives. Agric. For. Meteorol. 276-277, 107609. https://doi.org/10.1016/j.agrformet.2019.06.008.

Huang, M., Wang, J., Wang, B., Liu, D.L., Qiang, Y.u., He, D.i., Wang, N.a., Pan, X., 2020. Optimizing sowing window and cultivar choice can boost China's maize yield under 1.5 °C and 2 °C global warming. Environ. Res. Lett. 15 (2), 024015 https://doi.org/10.1088/1748-9326/ab66ca.

Jain, M., Srivastava, A., Balwinder-Singh, R.J., McDonald, A., Royal, K., Lisaius, M., Lobell, D., 2016. Mapping smallholder wheat yields and sowing dates using micro-satellite data. Remote Sens. (Basel) 8 (10), 860. https://doi.org/10.3390/rs8100860.

Jones, J.W., Hoogenboom, G., Porter, C.H., Boote, K.J., Batchelor, W.D., Hunt, L.A., Wilkens, P.W., Singh, U., Gijsman, A.J., Ritchie, J.T., 2003. The DSSAT cropping system model. Eur. J. Agron. 18 (3–4), 235–265. https://doi.org/10.1016/S1161-0301(02)00107-7.

Keating, B.A., Carberry, P.S., Hammer, G.L., Probert, M.E., Robertson, M.J., Holzworth, D., Huth, N.I., Hargreaves, J.N.G., Meinke, H., Hochman, Z., McLean, G., Verburg, K., Snow, V., Dimes, J.P., Silburn, M., Wang, E., Brown, S., Bristow, K.L., Asseng, S., Chapman, S., McCown, R.L., Freebairn, D.M., Smith, C.J., 2003. An overview of APSIM, a model designed for farming systems simulation. Eur. J. Agron. 18 (3–4), 267–288.

Lawlor, D.W., Tezara, W., 2009. Causes of decreased photosynthetic rate and metabolic capacity in water-deficient leaf cells: a critical evaluation of mechanisms and integration of processes. Ann. Bot. 103 (4), 561–579. https://doi.org/10.1093/aob/mcn244.

Li, Y., Guan, K., Schnitkey, G.D., DeLucia, E., Peng, B., 2019. Excessive rainfall leads to maize yield loss of a comparable magnitude to extreme drought in the United States. Glob. Chang. Biol. 25 (7), 2325–2337. https://doi.org/10.1111/gcb.14628.

Li, J., Roy, D., 2017. A global analysis of sentinel-2A, sentinel-2B and landsat-8 data revisit intervals and implications for terrestrial monitoring. Remote Sens. (Basel) 9 (9), 902. https://doi.org/10.3390/rs9090902.

Liu, L., Cao, R., Chen, J., Shen, M., Wang, S., Zhou, J.i., He, B., 2022. Detecting crop phenology from vegetation index time-series data by improved shape model fitting in each phenological stage. Remote Sens. Environ. 277 (August), 113060 https://doi.org/10.1016/j.rse.2022.113060.

Lobell, D.B., Ivan Ortiz-Monasterio, J., Sibley, A.M., Sohu, V.S., 2013. Satellite detection of earlier wheat sowing in India and implications for yield trends. Agr. Syst. 115 (February), 137–143. https://doi.org/10.1016/j.agsy.2012.09.003.

Mandrini, G., Archontoulis, S.V., Pittelkow, C.M., Mieno, T., Martin, N.F., 2022. Simulated dataset of corn response to nitrogen over thousands of fields and multiple years in Illinois. Data Brief 40 (February), 107753. https://doi.org/10.1016/j.dib.2021.107753.

Migliavacca, M., Galvagno, M., Cremonese, E., Rossini, M., Meroni, M., Sonnentag, O., Cogliati, S., Manca, G., Diotri, F., Busetto, L., Cescatti, A., Colombo, R., Fava, F., Morra di Cella, U., Pari, E., Siniscalco, C., Richardson, A.D., 2011. Using digital repeat photography and eddy covariance data to model grassland phenology and photosynthetic CO2 uptake. Agric. For. Meteorol. 151 (10), 1325–1337. https://doi.org/10.1016/j.agrformet.2011.05.012.

Morel, J., Parsons, D., Halling, M.A., Kumar, U., Peake, A., Bergkvist, G., Brown, H., Hetta, M., 2020. Challenges for simulating growth and phenology of silage maize in a nordic climate with APSIM. Agronomy 10 (5), 645. https://doi.org/10.3390/agronomy10050645.

Moulin, S., Kergoat, L., Viovy, N., Dedieu, G., 1997. Global-scale assessment of vegetation phenology using NOAA/AVHRR satellite measurements. J. Clim. 10 (6), 1154–1170. https://doi.org/10.1175/1520-0442(1997)010<1154:GSAOVP>2.0.CO;2.

Nemergut, K.T., Thomison, P.R., Carter, P.R., Lindsey, A.J., 2021. Planting depth affects corn emergence, growth and development, and yield. Agron. J. 113 (4), 3351–3360. https://doi.org/10.1002/agj2.20701.

Papale, D., Reichstein, M., Canfora, E., Aubinet, M., Bernhofer, C., Longdoz, B., Kutsch, W., et al., 2006. Towards a more harmonized processing of eddy covariance CO2 fluxes: algorithms and uncertainty estimation. Biogeosci. Discuss. Euro. Geosci. Union. https://doi.org/10.5194/bgd-3-961-2006.

Peng, B., Guan, K., Chen, M., Lawrence, D.M., Pokhrel, Y.d., Suyker, A., Arkebauer, T., Yaqiong, L.u., 2018. Improving maize growth processes in the community land model: implementation and evaluation. Agric. For. Meteorol. 250–251 (March), 64–89. https://doi.org/10.1016/j.agrformet.2017.11.012.

Phan, H., Le Toan, T., Bouvet, A., Nguyen, L., Duy, T.P., Zribi, M., 2018. Mapping of rice varieties and sowing date using X-band SAR data. Sensors 18 (2), 316. https://doi.org/10.3390/s18010316.

Plancade, S., Marchadier, E., Huet, S., Ressayre, A., Noûs, C., Dillmann, C., 2022. A new hypothesis-testing model for phyllochron based on a stochastic process - application to analysis of genetic and environment effects in maize. bioRxiv. https://doi.org/10.1101/2021.01.11.426247.

Sacks, W.J., Kucharik, C.J., 2011. Crop Management and phenology trends in the U.S. corn belt: impacts on yields, evapotranspiration and energy balance. Agric. For. Meteorol. 151 (7), 882–894. https://doi.org/10.1016/j.agrformet.2011.02.010.

Sadeh, Y., Zhu, X., Dunkerley, D., Walker, J.P., Zhang, Y., Rozenstein, O., Manivasagam, V.S., Chenu, K., 2021. Fusion of sentinel-2 and planetscope time-series data into daily 3 m surface reflectance and wheat LAI monitoring. Int. J. Appl. Earth Obs. Geoinf. 96, 102260. doi.org/10.1016/j.jag.2020.102260.

Sakamoto, T., 2018. Refined shape model fitting methods for detecting various types of phenological information on major U.S. Crops. ISPRS J. Photogramm. Remote Sens. 138 (April), 176–192. https://doi.org/10.1016/j.isprsjprs.2018.02.011.

Sakamoto, T., Wardlow, B.D., Gitelson, A.A., Verma, S.B., Suyker, A.E., Arkebauer, T.J., 2010. A two-step filtering approach for detecting maize and soybean phenology with time-series MODIS data. Remote Sens. Environ. 114 (10), 2146–2159. https://doi.org/10.1016/j.rse.2010.04.019.

Schnitkey, G., Swanson, K., Coppess, J., Paulson, N., 2020. 2020 planting decisions in the face of COVID-19. Farmdoc Daily 10 (49). https://farmdocdaily.illinois.edu/2020/03/2020-planting-decisions-in-the-face-of-covid-19.html.

Schwartz, M.D., Reed, B.C., White, M.A., 2002. Assessing satellite-derived start-of-season measures in the conterminous USA. Int. J. Climatol. 22 (14), 1793–1805. https://doi.org/10.1002/joc.819.

Seo, B., Lee, J., Lee, K.-D., Hong, S., Kang, S., 2019. Improving remotely-sensed crop monitoring by NDVI-based crop phenology estimators for corn and soybeans in Iowa and Illinois, USA. Field Crop Res 238 (May), 113–128. https://doi.org/10.1016/j.fcr.2019.03.015.

Shew, A.M., Tack, J.B., Nalley, L.L., Chaminuka, P., 2020. Yield reduction under climate warming varies among wheat cultivars in south africa. Nat. Commun. 11 (1), 4408. https://doi.org/10.1038/s41467-020-18317-8.

Sun, Z., Di, L., Fang, H., Burgess, A., 2020. Deep learning classification for crop types in North Dakota. IEEE J. Sel. Top. Appl. Earth Obs. Remote Sens. 13, 2200–2213. https://doi.org/10.1109/JSTARS.2020.2990104.

Thornton, P. E., Thornton, M. M., Mayer, B. W., Wei, Y., Devarakonda, R., Vose, R. S., Cook, R. B. 2016. Daymet: Daily Surface Weather Data on a 1-Km Grid for North America, Version 3. ORNL DAAC, Oak Ridge, Tennessee, USA. 2017 Census of Agriculture, Summary and State Data, Geographic Area Series.

Thornton, M.M., Shrestha, R., Wei, Y., Thornton, P.E., Kao, S-C., and Wilson, B.E. 2022. DaymetDaymet: Annual Climate Summaries on a 1-Km Grid for North America, Version 4 R1. NetCDF, GTiff, 0 MB. https://doi.org/10.3334/ORNLDAAC/2130.

Vijaya Kumar, P., Bal, S.K., Dhakar, R., Sarath Chandran, M.A., Subba Rao, A.V.M., Sandeep, V.M., Pramod, V.P., Malleswari, S.N., Sudhakar, G., Solanki, N.S., Shivaramu, H.S., Lunagaria, M.M., Dakhore, K.K., Londhe, V.M., Singh, M., Kumari, P., Subbulakshmi, S., Manjunatha, M.H., Chaudhari, N.J., 2021. Algorithms for weather-based management decisions in major Rainfed crops of India: validation using data from multi-location field experiments. Agron. J. 113 (2), 1816–1830. https://doi.org/10.1002/agj2.20518.

Vyas, S., Nigam, R., Patel, N.K., Panigrahy, S., 2013. Extracting regional pattern of wheat sowing dates using multispectral and high temporal observations from indian geostationary satellite. J. Indian Soc. Remote Sens. 41 (4), 855–864. https://doi.org/10.1002/agj2.20518.

Waha, K., van Bussel, L.G.J., Müller, C., Bondeau, A., 2012. Climate-driven simulation of global crop sowing dates: simulation of global sowing dates. Glob. Ecol. Biogeogr. 21 (2), 247–259. https://doi.org/10.1111/j.1466-8238.2011.00678.x.

Wang, S., Azzari, G., Lobell, D.B., 2019. Crop type mapping without field-level labels: random forest transfer and unsupervised clustering techniques. Remote Sens. Environ. 222 (March), 303–317. https://doi.org/10.1016/j.rse.2018.12.026.

Waongo, M., Laux, P., Traoré, S.B., Sanon, M., Kunstmann, H., 2014. A crop model and fuzzy rule based approach for optimizing maize planting dates in Burkina Faso, West Africa. J. Appl. Meteorol. Climatol. 53 (3), 598–613. https://doi.org/10.1175/JAMC-D-13-0116.1.

Way, D.A., Yamori, W., 2014. Thermal acclimation of photosynthesis: on the importance of adjusting our definitions and accounting for thermal acclimation of respiration. Photosynth. Res. 119 (1–2), 89–100. https://doi.org/10.1007/s11120-013-9873-7.

Westgate, M.E., Forcella, F., Reicosky, D.C., Somsen, J., 1997. Rapid canopy closure for maize production in the Northern US corn belt: radiation-use efficiency and grain yield. Field Crop. Res. 49 (2–3), 249–258. https://doi.org/10.1016/S0378-4290(96)01055-6.

Wu, C., Peng, D., Soudani, K., Siebicke, L., Gough, C.M., Arain, M.A., Bohrer, G., Lafleur, P.M., Peichl, M., Gonsamo, A., Xu, S., Fang, B., Ge, Q., 2017. Land surface phenology derived from normalized difference vegetation index (NDVI) at global FLUXNET sites. Agric. For. Meteorol. 233, 171–182. https://doi.org/10.1016/j.agrformet.2016.11.193.

Yang, Z., Diao, C., Li, B.o., 2021. A Robust hybrid deep learning model for spatiotemporal image fusion. Remote Sens. (Basel) 13 (24), 5005. https://doi.org/10.3390/rs13245005.

Zeng, L., Wardlow, B.D., Wang, R., Shan, J., Tadesse, T., Hayes, M.J., Li, D., 2016. A hybrid approach for detecting corn and soybean phenology with time-series MODIS data. Remote Sens. Environ. 181 (August), 237–250. https://doi.org/10.1016/j.rse.2016.03.039.

Zeng, L., Wardlow, B.D., Xiang, D., Shun, H.u., Li, D., 2020. A review of vegetation phenological metrics extraction using time-series, multispectral satellite data.

Remote Sens. Environ. 237 (February), 111511 https://doi.org/10.1016/j.rse.2019.111511.
Zhang, M., Abrahao, G., Cohn, A., Campolo, J., Thompson, S., 2021. A MODIS-based scalable remote sensing method to estimate sowing and harvest dates of soybean crops in Mato Grosso, Brazil. Heliyon 7, e07436. https://doi.org/10.1016/j.heliyon.2021.e07436.
Zhang, X., Friedl, M.A., Schaaf, C.B., Strahler, A.H., Hodges, J.C.F., Gao, F., Reed, B.C., Huete, A., 2003. Monitoring vegetation phenology using MODIS. Remote Sens. Environ. 84 (3), 471–545. https://doi.org/10.1016/S0034-4257(02)00135-9.
Zhang, X., Wang, J., Henebry, G.M., Gao, F., 2020. Development and evaluation of a new algorithm for detecting 30 m land surface phenology from VIIRS and HLS time series. ISPRS J. Photogram. Rem. Sens. 161 (March), 37–51. https://doi.org/10.1016/j.isprsjprs.2020.01.012.
Zhu, Z., Tao, Y., Luo, X., 2022. HCNNet: a hybrid convolutional neural network for spatiotemporal image fusion. IEEE Trans. Geosci. Remote Sens. 60, 1–16. https://doi.org/10.1109/TGRS.2022.3177749.